Weathering action on thermo-viscoelastic properties of polymer interlayers for laminated glass

Laura Andreozzi[1], Silvia Briccoli Bati[2], Mario Fagone[2], Giovanna Ranocchiai[2], Fabio Zulli[1]

[1]*Department of Physics 'Enrico Fermi', University of Pisa, largo Bruno Pontecorvo 3, 56127 Pisa, Italy*

[2]*Department of Civil and Environmental Engineering, University of Florence, piazza F. Brunelleschi 6, 50121 Florence, Italy*

phone +390552756830

fax +39055212083

giovanna.ranocchiai@unifi.it

Abstract.

Mechanical properties of interlayer polymers are recognized to be essential for a correct design of laminated glass structures. Although several researches have been carried out on the consequences of weathering actions on laminated glass, few quantitative data on the properties of polymers are available. The response of structures to long duration load is therefore evaluated taking into account the effects of viscosity of interlayer, but in the hypothesis that the interlayer material does not degrade over time. In this paper the results are reported of an experimental analysis of the thermo-viscoelastic properties of polyvinyl butyral used as interlayer of laminated glass, subjected to weathering actions (humidity, thermal cycles and UV radiation). The results were interpreted in the light of the connection between microstructure and rheology of polymers, and highlight two different damage mechanisms, promoted in different extents by the different weathering actions

Keywords: laminated glass, polymer interlayer, thermo-viscoelasticity, linear viscoelasticity, polyvinyl butyral, weathering, damage.

1. Introduction

Contemporary architecture is increasingly using structural glass, usually in the form of laminated glass sheets [1], often assembled with other materials [2], in order to reduce the consequences of glass fragility and to confer toughness to the structural element. The necessity of evaluating the mechanical response of such structural elements has required, first of all, the development of calculation methods for laminated glass [3, 4]. Considering that, in structural usages, glass

always remains in the linear elastic range up to brittle failure, simplified approaches are used to describe a generic laminated glass plate as a laminated composite made of elastic phases. In this way, laminated glass can be modelled using generalized Newmark models [5], widely employed for schematizing such phenomena, in case of composite elements made of other materials as, for example, steel–concrete interactions in reinforced concrete [6].

In view of the design of laminated glass structures, both a simplified prediction and a careful description of mechanical behavior of structural elements can be faced only if an accurate knowledge of the thermo-viscoelastic response of interlayer polymer is available [3, 4]. For this purpose, the authors have already proposed an experimental procedure for carrying out dynamic tests on small dimension laminated glass specimens, that permits to overcome some difficulties and some inconsistencies of the tests on polyvinyl butyral (PVB) interlayer [7]. As the coupling capability of interlayer is not negligible, [4, 8], weathering can significantly modify the structural response of laminated glass structures. For this reason, a comprehensive description of material behavior subjected to long time load conditions requires both a constitutive model, that accounts for the duration of the solicitation and refers to the material as it is at the moment of the experimental analysis, and the evaluation of the modifications of its properties due to weathering. In particular, environmental actions as temperature variations, solar radiation and diffusion of chemicals, usually acting on layered glass structures, can affect interlayer mechanical properties [9, 10].

Many studies reported in the literature are able to demonstrate significant influence of weathering on physical and mechanical properties of PVB, extensively used as interlayer in laminated glass. Some authors applied at the evaluation of the consequences of environmental degradation of PVB from a chemical point of view: Saad et al. [10] measured dielectric parameters and dynamic mechanical properties of PVB after different time exposure to UV radiation; El-Din and Sabaa [9] investigated the causes of thermal degradation of PVB; Liu [11] analyzed the problem of thermal stability of PVB and possible stabilization by adding various bases. Also international standard [12] proposes test methods to reproduce weathering action on laminated glass, focusing on thermal stability, UV radiation effect and consequences of absorption of moisture; however, the tests are mainly concerned with the visual consequences of the

exposure action rather than on the consequences on the mechanical properties or on the inner structure of material.

Some researchers, instead, are more interested on the consequences of weathering on the mechanical properties of laminated glass interlayer, as the expected behavior of the composite structure over the years could be unrealistic if the effects of solar radiation or of moisture diffusion are neglected. Delincé et al. [13] summarized the results obtained by some researchers on laminated glass subjected to UV radiation and moisture diffusion; Ensler [14] reported the results of mechanical monotonic tests on laminated glass specimens subjected to UV radiation, moisture diffusion and temperature variation, but the results are merely qualitative. Weller and Kothe [15] and, successively, Kothe and Weller [16] reported the results of a wide and systematic experimental investigation on glass laminated with PVB, EVA, TPU or ionomeric interlayer, even with combinations of environmental actions; however only rough results are reported in these papers, and the interpretation in the light of a thermo-viscoelastic model of material behavior is not carried out.

Louter et al. [17] focused their attention on the consequences of thermal and moisture action on the interface of ionomeric interlayer, in fact they perform pull out tests. Also Butchart and Overend [18] directed their attention on adhesion, but their research is mainly concerned with the different behavior of laminated glass interface in different ambient state, not as a consequence of different past situations. Serafinavicious et al. [19] reported the results of an extensive experimental analysis performed on glass laminated with ionomeric, EVA and PVB interlayers as a consequence of moisture exposure, UV radiation and combinations; four point creep bending tests have been performed at different temperature, but the results have not been elaborated as to represent the mechanical parameters of interlayer.

In spite of a rather large amount of experimental results, a comparison among them has not been attempted; indeed the methods used to reproduce weathering action in the laboratories are different and are aimed to study in turn the bulk properties of material, the adhesion properties or the consequences of diffusion from the edges of the structural element; moreover the methods used for the mechanical tests are different [20] and they are often used only for a qualitative comparison rather than for the analytical description of mechanical parameters.

In this paper, the results of experimental tests on the thermo-viscoelastic properties of laminated glass specimens are reported, after the action of weathering was simulated on them. In particular, the thermo-viscoelastic theories for polymers are reviewed in the second section; the experimental program, consisting of both the weathering procedures and the mechanical tests, are presented in the third section; the results of mechanical tests are reported in the fourth section and in the fifth section they are compared with the results obtained on specimens extracted from the same laminated glass elements, not subjected to any treatments. Finally, the conclusions are drawn in the last section. The test procedure already perfected for the mechanical analysis of laminated glass specimens revealed particularly apt to the analysis of specimens subjected to artificial weathering, because it permits to perform the tests directly on laminated glass specimens, so that the environmental action is effectively produced on interlayer inside the composite glass, as it is in the reality.

2. Thermo-viscolelasticity in polymers

The mechanical properties of the polymers employed as interlayer in laminated glass can be described by recurring to main tools handling the linear viscoelasticity, because interlayers are generally isotropic and linear elastic, before to be subjected to significant strain; moreover, they are usually assumed as incompressible materials [21].

The Boltzmann superposition principle [22] is generally adopted to describe the viscoelastic behaviour of isotropic polymers in the range of linear response. Accordingly, every mechanical load step provides an independent contribution to the total mechanical history so that the final response of the material is the sum of the response at each step.

Consequently, for experiments carried out in simple shear mode, the time dependence of the strain γ can be expressed as an integral involving the creep compliance *J(t)* and the rate of shear stress $\dot{\tau}$ [23]:

$$\gamma(t) = J(t)\tau(0) + \int_0^t J(t-t')\dot{\tau}(t')dt' \quad (1)$$

In equation (1) it is assumed that the load history starts at time $t = 0$.

Likewise, the time dependence of the shear stress can be expressed as an integral involving the shear relaxation modulus *G(t)* and the shear rate $\dot{\gamma}$ [23]:

$$\tau(t) = G(t)\gamma(0) + \int_0^t G(t-t')\dot{\gamma}(t')dt' \quad (2)$$

Test methods for the time dependent mechanical behaviours of the materials of interest in this work, are characterized by specific ranges of load rates [24], pertain to specific time and frequency domains, and refer to the linear viscoelastic regime.

Typical transient experiments are the creep and the stress relaxation [22, 25, 26]. In creep experiments, a constant shear stress τ is suddenly applied to a specimen and the shear strain $\gamma(\tau)$ is registered as a function of time (see Eq. (1)), so that the creep compliance is evaluated from the experiment as $J(t) = \gamma(t)/\tau$ [27, 28]. Similarly, in stress relaxation experiments, a constant strain γ is suddenly imposed to a specimen and the corresponding stress $\tau(t)$ is determined, so obtaining the shear relaxation modulus $G(t)=\tau(t)/\gamma$ (Eq. (2)). Note that *G(t)* and *J(t)* are not reciprocal functions because they represent the response to different experimental load histories. More simply, the relaxation modulus *G(t)* can be directly used to simulate the behaviour of a body subjected to an imposed displacement for a time *t* on the boundary, while the creep compliance *J(t)* can be directly used to simulate the behaviour of material subjected to an imposed stress for a time *t* on the boundary.

If stress (or strain) applied on a linear viscoelastic material is varied in a sinusoidal way with angular frequency ω, the strain (or stress) also oscillates with the same law and frequency, but it will be out of phase by an angle δ, namely the damping angle [22, 26]. For sufficiently small deformations, material functions such as relaxation modulus or creep compliance are independent of the amplitude of strain or stress applied to the specimen. For a sinusoidal strain

$$\gamma(t) = \gamma_0 \sin \omega t \quad (3)$$

the stress can be expressed as [22 p. 12]

$$\tau(t) = \tau_0 (G' \sin \omega t + G'' \sin \omega t) \quad (4)$$

where the shear storage modulus $G'(\omega)$ and the shear loss modulus $G''(\omega)$ are functions of the material and the angular frequency only.

After representing as complex quantities the sinusoidal strain and stress

$$\gamma^* = \gamma_0 \exp(i\omega t) \quad ; \quad \tau^* = \tau_0 \exp(i\omega t + i\delta) \tag{5}$$

(i^2 = -1), measurements of the amplitude of the shear stress t_0, strain g_0 and of phase angle δ provide [25] the complex shear modulus $G^*(\omega)=G'+iG''$, and its reciprocal, the complex compliance $J^*(\omega)$, according to the definitions:

$$G^*(\omega) = \frac{\tau^*}{\gamma^*} = \frac{1}{J^*(\omega)} \tag{6}$$

The linear viscoelastic equations (1), (2) and (6) are interrelated through exact analytical relations, provided that the constitutive behaviour is known over a sufficiently wide range of time or frequencies [22].

The values of $G'(\omega)$ and $G''(\omega)$, as well as on the angular frequency ω, also depend on the temperature T. For many polymer materials, it was observed that the experimental $G^*(\omega)$ curves, obtained at a given temperature, might be shifted in a logarithmic time scale to superimpose to experimental points obtained at a different temperature [23, 25]. In this case, one says that the Time-Temperature Superposition (TTS) principle is valid over a given range of angular frequency ω and temperature T. Then, in particular, the frequency sweeps recorded at certain temperatures T can be superimposed on a single master curve at a reference temperature T_r by vertical $b_{Tr}(T)$ and horizontal $a_{Tr}(T)$ shifts according to

$$G^*(\omega,T) = b_{Tr}(T)\, G^*(a_{Tr}(T)\, \omega, T_r) \tag{7}$$

Eq. (7) implies that the material function $G^*(\omega)$ at T_r can be plotted over a frequency domain larger than the available one from the instrument. When TTS holds, and $b_{Tr}(T) \cong 1$, a general form for the description of $a_{Tr}(T)$ as a function of T, also derived in the framework of free-volume theories (see [29, 30] and references therein), was proposed by William, Landel and Ferry (WLF equation):

$$\log a_{Tr}(T) = -\frac{C_1(T - T_r)}{C_2 + T - T_r} \tag{8}$$

The knowledge of the C_1 and C_2 constants allows the shifting of the master curve at different temperatures. However, care should be paid in attempting to predict

properties at frequencies or times many decades far from the range of experimental measurements, because of accumulation of experimental errors and, also, of chemical and structural changes that may occur in the material over long time periods.

It is known that the macromolecular dynamics of high polymers is well accounted for by the tube theories, where the fundamental parameter describing the topological polymer network is the molecular weight between entanglements M_e [31]. In other words, M_e is the average molecular weight between temporary cross-links. There are two parameters linked to M_e: the basic time scale parameter τ_e, which is the equilibration time of the chain segment between entanglements, and the basic stress scale parameters, which is the plateau modulus G_N^0.

M_e and G_N^0 are unambiguously related each other in the tube picture [29]. One has [32]

$$M_e = \frac{4}{5}\frac{\rho RT}{G_N^0} \tag{9}$$

being ρ the density and R the molar gas constant.

From this relationship one can conclude that a measurement of G_N^0 provides information on the entanglement mass of the material. Moreover, G_N^0 is unaffected by the sample molecular mass M and its distribution, provided that the molecular weight is few times higher than M_e.

The time τ_e is related to the microscopic properties of the polymer according to

$$\tau_e = \tau_R \frac{M_e^2}{M} \tag{10}$$

being M the polymer mass and τ_R the Rouse time [29], defined as

$$\tau_R = \frac{\zeta_0 M^2 b^2}{3\pi^2 M_0^2 k_B T} \tag{11}$$

In the formula, ζ_0 is the monomeric friction coefficient, M_0 the mass of the monomer, k_B the Boltzmann constant and b a length proper of the specific polymer [33]

3 Experimental program

3.1 Weathering

Two two-ply composite glasses, having dimensions 400×300 mm and thickness 8-0.76-8 mm and 8-1.52-8 mm respectively, were laminated with PVB interlayer (Trosifol® BG R20) by Roberglass Srl (Calci, Pisa, Italy). Cylindrical specimens with diameter 23.06 mm were drilled by a grass core bit. Specimens obtained from 8-0.76-8 mm panes were marked with the letter A while specimens obtained from 8-1.52-8 mm were marked with the letter B. From each laminated glass ply, one cylindrical specimen was tested in order to determine the viscoelastic properties of blank material, to be used as a comparison, while other specimens were subjected to accelerated weathering action. International standard UNI EN ISO 12543-4:2011 (Laminated glass and laminated safety glass - Test methods for durability [12]) was taken as a reference for the definition of the artificial weathering procedures. However, it must be noted that UNI EN ISO 12543-4 aims at determine eventual appearance of faults (bubble, delamination, haze and cloudiness) that can be observed at a visual inspection at a distance of 300-500 mm, do not aim at determining eventual modifications in the mechanical response of laminated glass. For this reason, since the experimental program described in this paper is devoted to the analysis of the mechanical properties of the material, the standard was not followed when defining the dimensions and shape of specimens but they were defined in view of the successive dynamic mechanical tests.

The specimens were divided into three groups: the first group (named with letter U) was subjected to moisture action; the second group (named with letter T) was subjected to temperature cycles and the third group was subjected to UV radiation (named with letter I).

The action of moisture, of temperature cycles and of solar radiation were reproduced in laboratory so as to obtain effects that can be observed in the real lifetime of a laminated glass structure. This is not a trivial task, as shown by Martin et al. [34]; moreover, it must be kept in mind that the exposure of a laminated glass element can lead to very different situations depending on the latitude of the building, on its functionality, on the location and slope of the individual glass pane.

3.1.1 Temperature cycles

In programming the weathering procedures, attention has been paid to reproduce weathering actions that can occur during the life of the structural element. In this extent, prEN 16612 [35] considers for permanent loads a conservative maximum value for temperature of 60° C. Supposing that a constant temperature cannot be maintained in real architectures during lifetime and presuming that alternating temperature could induce alternating stresses that damage material more than a constant temperature, temperature cycles were planned. The temperature cycle extended for a period of four hours in the range between 10 and 50° C, so that it comprehended the glass transition temperature of PVB, (about 20°C); the temperature history is reported in Figure 1. In particular, two specimens were subjected to 114 cycles (T7A and T8B), two specimens were subjected to 202 cycles (T6A and T7B) and eleven specimens were subjected to 568 cycles (specimens from T1A to T5A and from T1B to T6B). These conditions can be easily obtained in glass roofing and skylight, where laminated glass panes separate indoors to outdoors; moreover, temperature can effectively pass from below to above 20°C in the transition from night to day and vice versa, in the middle seasons, so that we can presume that the proposed cycle numbers can be representative of the thermal weathering of many structures during one or more years of life.

3.1.2 Humidity action

Specimens subjected to moisture action were kept suspended over a covered thermostatic bath at the temperature of 50°C. These conditions give a relative humidity of about 100% and lead to water condensing on the surface of the test specimens. The specimens were maintained in this state for 456 hours (U7A and U8B), for 809 hours (U6A and U7B) and for 5425 hours (specimens from U1A to U5A and from U1B to U6B). Accelerated moisture damage can hardly be compared to some environmental conditions; a so long exposure to humidity can be reached in case of structural elements of very wet buildings, such as swimming pools, or at the open air in very wet climates. Moreover, it must be considered that the diffusion of humidity proceeds from the boundary to the centre of the specimens; small specimens are characterized by a very high edge to bulk rate and are therefore very sensitive to the action of moisture, with respect to large

specimens and to real structural elements. However, the choice of very severe conditions permits to measure any eventual consequences of extreme moisture action.

3.1.3 Radiation action

Specimens were kept in front of a lamp Ultra-Vitalux® 300W (Osram) at a distance of 25 cm; the spectrum of radiation produced is considered well reproduce the spectrum of sun radiation. It has been verified that the temperature of the specimens did not overcome 35°C during the weathering procedure. Comparing with the condition proposed in UNI EN ISO 12543-4, the distance from the radiation source combined with the overlapping of the light beams suggests that the total irradiance level in the plane of the test is, as in UNI EN ISO 12543-4, 900±100 W/m^2. The specimens were maintained in this state for 912 hours (I8A and I8B), for 7968 hours (I1A) and for 11209 hours (from I2A to I7A and from I1B to I7B). Considering that the total radiation on a sloping surface facing south in Florence (Italy) during one year is about 1602 kWh/m^2 [1], such exposition times correspond respectively to 6 average months, to more than 4 years, and to about 6 years on a roofing in Florence (Italy) facing south.

3.2 Visual analysis

Before performing mechanical tests, the specimens subjected to weathering actions were inspected in order to detect eventual faults.

Specimens subjected to thermal cycles showed no apparent signs of damage.

Specimens subjected to humidity showed the consequences of water (or vapour) diffusion: moisture diffused progressively over time, from the boundary towards the centre of the cylindrical specimens. After 809 hours, (about 33 days) specimens were opaque for some millimetres, while after 5425 hours (more than 7 months) they were completely opaque (Figure 2). Specimens to be subjected to mechanical tests were conditioned at room temperature and humidity till they recovered the original transparency (Figure 3a). It was necessary 1 month and 6

[1] The total solar radiation was evaluated with the interactive software made by Italian Agency ENEA http://www.solaritaly.enea.it/CalcRggmmIncl/Calcola.php according to UNI 8477/1 "Calcolo degli apporti per applicazioni in edilizia. Valutazione dell'energia raggiante ricevuta".

months respectively to recover the transparency. Three of the specimens 8-0.76-8 mm were also affected by delamination, from the boundary towards the centre Figure 3b. Specimens U4A and U5A have been selected to perform the mechanical tests; for this reason, evaluating the delaminated area was necessary. The photos (taken with Canon EOS 400D camera, EF100mm f2.8 macro lens) of the specimen before and after the delamination phenomenon were compared and the percentage of delaminated area was evaluated using an image manipulation program. In the following, the effective mechanical response of the U4A and U5A specimens has been determined including the contribution of delamination at first, then the *true* rheological properties of the PVB interlayer have been obtained considering a reduced area, namely referring to circular cylinders of equivalent area.

Specimens subjected to solar radiation for long time showed evident modification in colour: PVB assumed a marked yellow colour, as it can be noted in Figure 4.

3.3 Mechanical tests

Mechanical tests were carried out on A specimens, since the specimens made of PVB with a thickness of 0.76 mm seemed to show greater influence of damage; the weathering action imposed to the tested specimens is summarized in Table 1. The results were compared with those obtained on a blank specimen (PVB@0.76) already tested, whose behaviour was described in [36].

Oscillatory tests have been performed on the specimens, according to the procedure extensively reported in [7]. Rheological measurements were carried out, by using an Anton Paar MCR Physica^{TM} 301 rheometer, equipped with CTD 450 temperature control unit, with parallel plate geometry. For adhesion purposes, the round glass surfaces of the specimens (the bases of the cylinder) were connected to the load plates of the rheometer with a proper glue (Vitralit® 6128 Panacol-Elosol GmbH).

Frequency sweep experiments were carried out, for various frequency intervals and at temperatures in the range 25- 65 °C, as reported in Table 2.

The adopted geometry for the experiments did not allow to reveal the G^* curves below 25°C for all the samples; for some of them it was even impossible until 28°C. This is ascribable to the glassy state of the PVBs, according to T_g values reported in the literature [37].

In order to ensure that the tests were carried out within the linear viscoelastic range, preliminary experiments were carried out at different values of strain γ_0, that showed linear response at least up to γ_0=0.5 %. Measurements were then performed at the angular deflection ϕ=0.141mrad corresponding to a 0.2% maximum shear strain.

The loss angle δ and the complex shear modulus magnitude $|G^*|$ were measured during the tests. It is worth noting that, because of the difference in stiffness between glass and polymer, the imposed displacement caused a deformation that can be reasonably attributed to the interlayer only. In so doing, the polymer interlayer is subjected to a pure shear strain and the influence of the surface adhesion to glass is taken into account appropriately.

Because of the specimen geometry, a corrective factor had to be applied to the measured G^* modulus in order to obtain G^*_{PVB}, as extensively discussed in [7]. In that paper, it has been shown that the shear modulus G^*_{PVB} of the interlayer can be evaluated according to

$$G^*_{PVB} = G^*_{sensor} \frac{d_{PVB}}{d_{comp}} \frac{R^4_{sensor}}{R^4_{glass}} \tag{12}$$

In eq. (12), R_{glass} is the radius of the cylindrical specimen, R_{sensor} the radius of the sensor, d_{comp} is the gap between the sensors of the rheometer (corresponding to the height of the cylindrical specimen), and d_{PVB} is the actual thickness of the interlayer. G^*_{sensor} is the complex modulus measured by the rheometer.

In the following of the manuscript, G^* together with all the related rheological material functions will be referring to the ones pertinent to PVB.

Table 1. Specimens intended for mechanical tests and type of weathering

Temperature cycles		Humidity action		Radiation action	
T7A	114 cycles	U7A	456 hours	I8A	912 hours
T6A	202 cycles	U6A	809 hours	I1A	7968 hours
T1A	568 cycles	U5A U4A	5425 hours	I2A	11209 hours

Table 2. Temperatures and frequencies for PVB specimens.

Temp. (°C)	Frequency (Hz)										
	@0.76	T7A	T6A	T1A	U7A	U6A	U4A	U5A	I8A	I1A	I2A
25	10^{-2}-10^{2}			10^{-2}-10^{0}				10^{-2}-10^{2}	10^{-2}-10^{0}	10^{-2}-10^{2}	
27		10^{-2}-10^{2}									
30	2.5 10^{-4} - 2.5 10	10^{-2}-10^{2}	10^{-2}-10^{2}	10^{-2}-10^{2}	10^{-2}-10^{2}	10^{-2}-10^{2}	10^{-2}-10^{2}	10^{-2}-10^{2}	10^{-2}-10^{2}	10^{-2}-10^{2}	10^{-2}-10^{2}
35		10^{-2}-10^{2}	10^{-2}-10^{2}	10^{-2}-10^{2}	10^{-2}-10^{2}			10^{-2}-10^{2}	10^{-2}-10^{2}	10^{-2}-10^{2}	
40	10^{-4}-10^{2}	10^{-2}-10^{2}	10^{-2}-10^{2}	10^{-2}-10^{2}	10^{-2}-10^{2}		10^{-2}-10^{2}		10^{-2}-10^{2}	10^{-2}-10^{2}	10^{-2}-10^{2}
45		10^{-2}-10^{2}	10^{-2}-10^{2}	10^{-2}-10^{2}	10^{-2}-10^{2}			10^{-2}-10^{2}	10^{-2}-10^{2}		
50	10^{-4}-10	10^{-2}-10^{2}	10^{-2}-10^{2}	10^{-2}-10^{2}	10^{-2}-10^{2}				10^{-2}-10^{2}	10^{-2}-10^{2}	10^{-2}-10^{2}
55			10^{-2}-10^{2}	10^{-2}-10^{2}	10^{-2}-10^{2}		10^{-2}-10^{2}		10^{-2}-10^{2}	10^{-2}-10^{2}	10^{-2}-10^{2}
60	10^{-4}-10^{2}		10^{-2}-10^{2}	10^{-2}-10^{2}	10^{-2}-10^{2}	10^{-2}-10^{2}		10^{-2}-10^{2}	10^{-2}-10^{2}	10^{-2}-10^{2}	10^{-2}-10^{2}
65		10^{-2}-10^{2}		10^{-2}-10^{2}	10^{-2}-10^{2}		10^{-2}-10^{2}		10^{-2}-10^{2}		10^{-2}-10^{2}

4. Results

4.1 Temperature cycles

The master curves of dynamic moduli G' and G'' of the specimens T1A, T6A and T7A are shown in Figure 5 at the reference temperature T_r=30°C. The horizontal and vertical shift factors $a_{Tr}(T)$ and $b_{Tr}(T)$ at the reference temperature T_r, as well as the master curves, are obtained in this work by mathematical shifting of experimental isotherm frequency sweeps of the complex modulus $G^*(\omega)$. By inspection, it appears that, within the investigated temperature range, the TTS principle was found to be applicable. Indeed, $b_{Tr}(T)$ was found about equal to 1 throughout the specimen series, while the temperature dependence of the horizontal shift factors $a_{Tr}(T)$ is well described by the semiempirical WLF law eq. (8). The values of the WLF parameters C_1 and C_2 at T_r for the temperature-weathered specimens are reported in Table 3.

It is seen that the values of the WLF parameters C_1 and C_2 are practically coincident, within the uncertainty, and independent of the thermal cycle imposed to the specimen. A calculation of the invariant $C_1 \times C_2$ [30] evidences that its value is compatible, within the errors, throughout the T-series and with the blank PVB. Interestingly enough, it is also consistent with literature results on PVB reported in [38 p. 457] that provides for the invariant $C_1 \times C_2$ the value 985 K.

The master curves reported in Figure 5 show that the rheological response of the interlayers is located in the rubbery dynamic region as the rubbery plateau clearly

dominates the master curves. Moreover, it is seen that the temperature oscillations of the thermal cycles in the range 10-50 °C do not alter appreciably the rheological response of the polymer interlayer, at least after 560 repetitions. In fact, the three dynamic moduli are virtually identical in shape and quite superimposable, as it is apparent from the figure.

A more refined analysis is provided by looking in details at the crossover frequency and plateau modulus values of the master curves.

The crossover frequency f_c roughly corresponds to the engagement time τ_e, which is a microscopic time, characteristic of entangled polymers, defined by equation (10). The blank PVB and the T7A sample have a crossover frequency f_c located at compatible values.

As previously discussed, τ_e depends only on the number of monomers competing to the strands of entanglement mass M_e and on the monomeric friction coefficient [31]. Therefore, the result could ensure that there have not been changes at the nanoscale within the material, at least after a hundred of cycles. After increasing the number of thermal cycles, in T1A f_c appears shifted towards a lower frequency, signalling an apparent decrease of the mobility of the polymer chain at the same temperature T_r, or an increase of the T_g of the interlayer, in accordance with the possibility of carrying out the rheological measurements at 25°C (see Table 2 and paragraph 3.3).

From the master curves, the plateau modulus G_N^0 can be experimentally determined by adopting the criterion of the minimum of tan $\delta = G''/G'$. At the frequency where tan δ is minimum [39, 40], one sets $G_N^0 = G'(\omega : \tan\delta \min)$ (see Figure 6 as an example referring to the specimen T1A) . Accordingly, the plateau modulus G_N^0 can be evaluated and, for all these three specimens, the values are reported in Table 3.

By inspection, apart from the T7A result, the other T-specimens and the blank PVB show comparable values for G_N^0. These values are in nice agreement with the ones of the G modulus reported in [37], after performing a Rivlin-Mooney analysis of tensile experiments carried out on PVB samples obtained from various manifacturers.

The equation 9 allows an estimation of M_e of PVB that gives M_e = 4.67 kg mol^{-1} for blank PVB. In the calculus the typical value ρ =1.065 g/cm^3 given for the

density of the Trosifol® BG R20 was assumed. In Table 3, the entanglement masses are calculated for the series of the temperature weathered specimens. The data are in good agreement both each other and with the blank PVB, with no marked differences also with the T7A case. Moreover, it is worth noting that the results on M_e fit with literature data [37], taking into account that in the present work the "G" definition of M_e is assumed (eq. 9), which produces a value of M_e that is only 4/5 as large as that of the "F" definition [32].

Table 3. Rheology parameters of the specimens: WLF parameters, invariant $C_1 \times C_2$, plateau modulus G_N^0, crossover frequency f_c of G' and G'' master curves and entanglement mass M_e

Specimen (exposure)	C_1	C_2 (K)	$C_1 \times C_2$ (K)	G_N^0 (MPa)	ν: min tanδ (Hz)	f_c (Hz)	M_e (kg mol^{-1})
T1A (568 cycles)	12±1	80±10	960±126	0.44	4.0 10^-4	0.36	4.89
T6A (202 cycles)	13±2	95±20	1236±292	0.45	6.5 10^-4	--	4.78
T7A (114 cycles)	13±1	100±15	1300±219	0.38	2.5 10^-4	0.86	5.66
U4A (5425 hours)	13±3	120±25	1560±485	0.38	2.5 10^-4	0.31	--
U4A rescaled	13±3	120±25	1560±485	0.60	2.5 10^-4	0.31	3.58
U5A (5425 hours)	13±2	95±20	1235±322	0.35	8.0 10^-4	0.55	--
U5A rescaled	13±2	95±20	1235±322	1.21	8.0 10^-4	0.55	1.78
U6A (809 hours)	10±2	65±15	650±198	0.50	3.0 10^-4	0.19	4.30
U7A (456 hours)	10±1	65±10	650±119	0.47	4.0 10^-4	0.32	4.57
I1A (7968 hours)	9±1	55±80	495±90	0.68	3.0 10^-4	--	3.16
I2A (11209 hours)	--	--	--	--	--	--	
I8A (912 hours)	11±1	80±10	880±117	0.43	8.0 10^-4	1.11	5.00
Blank PVB@0.76	12±1	90±10	1080±150	0.46	8.0 10^-4	0.75	4.67

4.2 Humidity action

The master curves of the dynamic moduli G' and G'' of the specimens U4A, U5A, U6A and U7A are shown in Figure 7 and Figure 8 at the reference temperature T_r=30°C. As previously pointed out, the specimens U4A and U5A, both subjected to weathering duration of 5425 hours, delaminated at the boundary so that, in order to obtain more reliable values on the effective damages on the PVB interlayer, it was necessary to rescale the corresponding dynamic moduli referring to the effective bonding area between glass and PVB interlayer. Particularly, the reduction of area produced by delamination was supposed to be distributed uniformly on the boundary of the circular specimens, so that bonded area of U4A

and U5A specimens was supposed to remain circular with a diameter of 20.03 and 16.98 mm respectively. Non-rescaled master curves of U4A and U5A specimens are reported in Figure 7 for purposes of comparison of the damage effects over the applicability and functionality of laminated structural elements, while rescaled values are reported in Figure 8. Specimens U6A and U7A did not show debonding so that they did not require rescaling.

The TTS principle appears to be applicable within the investigated temperature range also after humidity-weathering. The vertical shift factor $b_{Tr}(T)$ is found about 1 throughout the specimen series, and the temperature dependence of the horizontal shift factors $a_{Tr}(T)$ are well described by a WLF dependence. Table 3 reports the values of the WLF parameters C_1 and C_2 at T_r for U-specimens subjected to the humidity action for different durations, as well as the value of the invariant $C_1 \times C_2$. The rescaling procedure does not affect the WLF parameters and the invariant. In case of U6A and U7A samples, they do not fit the values assumed in blank PVB, while U4A and U5A show compatible, even if higher, values.

Regarding the master curves reported in Figure 7 and pertinent to the different weather treatments, it is seen that they are influenced by the damage action and do not appear superimposable each other. Seemingly, humidity action softens the dynamic response of the structural laminate glasses: the dynamic modulus G' appears to decrease with increasing weathering time and delamination.

Actually, it is apparent from Figure 8 that rescaling leads to coherent results, in which the effects of the degradation, following the exposure of the specimen to the humidity, can be analyzed in terms of the interlayer properties only. It results an overall increase of the stiffness of the PVB interlayer with the increase of weathering time, in agreement with previous literature observation [13].

Moreover, the crossover frequencies f_c diminish in value with the increase of the delamination of the specimen, confirming an overall seeming “more rigid” response of the interlayer.

4.3 Radiation action

The different effects over the specimens determined by the exposure to UV irradiation are shown by the master curves of dynamic moduli G' and G'' of the specimens I8A, I1A and I2A (Figure 9). In I8A (912 hours of exposition) and I1A (7968 hours of exposition) specimens TTS principle still maintains its validity, within the investigated temperature range. The vertical shift factor $b_{Tr}(T)$ was found about 1, and the temperature dependence of $a_{Tr}(T)$ is well described by WLF laws. Table 3 reports the values of the WLF parameters C_1 and C_2 at T_r=30°C for I8A and I1A and the invariant $C_1 \times C_2$. It is seen that their values are not in agreement each other, signalling that appreciable changes in the structural properties of the interlayer took place by effect of UV damage. As probably expected, the specimen I8A, with less exposure to artificial weathering, exhibits WLF parameters compatible with the one of blank PVB specimen.

Regarding I2A specimen (11209 hours of exposition), its rheological data reported in Figure 9 refer to a single frequency sweep recorded at T=30 °C, because TTS principle failed on this specimen exposed to UV irradiation for about 458 days. It appears therefore that UV is able to modify the inner structure of the PVB interlayer resulting firstly in changes of the properties of the structural relaxation of the material and finally in the failure of the thermorheological simplicity of the specimens. By inspection of Figure 9, it is also apparent that the different UV exposition times provide master curves of shear moduli of the polymer interlayers that differ in shape. In particular, the response of I8A exhibits the rubbery plateau, in accordance with the previous findings on the blank specimen. Instead, G' and G'' of specimens I1A and I2A present similar behaviours with the frequency, in which a power law dependence well describes the elastic dynamics of the specimens.

The power law exponents are found highly compatible over the two specimens resulting in the value of 0.18. Note that in the rubbery plateau region the exponent value is about zero.

In the I-specimens case, the plateau modulus G_N^0 can be experimentally determined for I8A. It is found G_N^0 = 0.43 MPa. The crossover frequency is also

available for I8A specimen, and is located to an higher value with respect to blank PVB, signalling an effective increase of the local mobility in the specimen.

The shape of the shear complex moduli of I1A allows an attempt to extract a plateau modulus value, providing G_N^0 = 0.68 MPa, a result that has to be considered with caution.

A more specific investigation on the damages determined by UV irradiation has to be planned, in order to enlighten probable different degradation mechanisms selectively altering the properties of both plasticizer and neat PVB polymer matrix.

5 Comparison among results

According to the results presented in this work, it can be argued that at least two different mechanisms of degradation affect the response of the weathered specimens: a macroscopic and a microscopic one.

The macroscopic one is the delamination that acted in an evident way over two U-specimens, whose effects were calculated and removed over the master curves (Figures 7 and 8).

The other mechanism can be investigated and described, by analysing some specific spectral details and parameters of the shear rheological response of most of the weathered specimens.

At first, we consider the behaviour of a parameter of interest in the study of the dynamic response of polymers, namely the steepness index, or dynamic fragility *m* [41, 42 p. 1222], defined as

$$m = \frac{C_1}{C_2} \cdot \frac{1}{\left(1 - \frac{T_r - T_g}{C_2}\right)^2} \tag{13}$$

It characterizes the changes in the physical properties of the material as it approaches T_g. When *m* is high, the material is referred to as a fragile one and when *m* is low it is a strong material [43].

m depends explicitly on the quantities of equation (13), but it is known that it can also exhibit a mass dependence [44, 45]. The dynamic fragility *m* is calculated after assuming the literature average value for T_g = 289K [37] and reported in Figure 10 for all the specimens of Table 3, excluding I2A where TTS fails. The average value of *m* = 57 is found. This finding supports the idea that the degradation processes proceed without including changes in the polymer mass of PVB, at least at its first stages.

Note that deviations are observed in U4A and I1A specimens, with a decrease and an increase with respect to the average *m*, respectively. According to literature findings on polymers [44, 46], this would suggest some activity of the degradation processes that would decrease (U4A) or increase (I1A) the molar mass of the interlayer.

More insight is provided by considering G_N^0 and the crossover frequency of the master curves. A more refined analysis of the evolution of G_N^0 with the weathering is given in the Figure 11, where G_N^0 is shown as a function of the pertinent crossover frequency $f_c \sim 1/\tau_e$.

In the figure, the rescaled G_N^0 values are reported for the U4A and U5A specimens. The line is pertinent to the power law of exponent 1/2 that relates G_N^0 and f_c as the entanglement mass varies, because of the inverse proportionality on M_e of G_N^0 and the dependence on the square of M_e of τ_e, in agreement with the tube theories of entangled polymers [31].

According to equations from (9) to (11), it appears that both G_N^0 and f_c are independent of the polymer mass. Therefore, no changes in the physico-chemical properties of the interlayer would imply that all the data collapse to a single point, namely the one pertinent to clean PVC. Indeed the samples characterised by the smallest amount of thermal and irradiation weathering appear in its proximity.

Apart from U5A, the others roughly distribute within a ribbon of G_N^0 values, parallel to the f_c axis, with nearly constant or very similar values. It is worth noting that the result, and then the degradation mechanism, apply to all the weathering procedure, including also the I-processes to a some extent.

According to the tube theories of entangled polymers [31] and equation (9), a constant G_N^0 would imply that M_e is almost constant in these specimens; so the degradation mechanisms at this stage could be rather associated to slight changes of number density, probably connected to the amount of plasticizer of the commercial PVB. At variance, U5A sample seems to be affected mainly by changes of entanglement concentration in the specimen. This latter mechanism could originate also the degradation of I1A and I2A samples, not considered in the figure.

By inspection of the Figure 11, the presence of a spread of about one decade over the values of the experimental f_c can be detected. Searching for quantities affecting the f_c value at a constant temperature T, it is recognised from equations (10) and (11) that a change of the friction coefficient ζ_0 is a possible mechanism able to shift the location of the crossover frequency in the master curve of the dynamic shear moduli [30]. In particular, changes are mostly foreseen in case of variations of T_g, as a consequence of variations in the microstructure of the interlayer, once again due to degradation processes acting at various extent on the local mobility of the PVB, for example altering the plasticizer content.

6 **Conclusions**

As a conclusion, we can concisely summarize the results already analysed in the previous paragraphs.

- Thermal cycles between 10 and 50°C do not significantly affect the mechanical response of PVB.
- Humidity action, in the intensity proposed, strongly influence both the adhesion properties and the bulk response of PVB.
- UV radiation, in the intensity proposed, strongly influences both the colour and the mechanical properties of PVB.
- Steepness index, plateau modulus, crossover frequency and the relation among these last parameters, have been analysed in order to interpret the degradation phenomena. The observation of these parameters supports the idea that the degradation mechanisms acting on U- and T- specimens are not related to changes of the entanglement concentration of the PVB interlayer, but rather to changes in the local mobility in the polymer as possible consequence of alteration in the plasticizer properties.

- From a practical point of view, degradation phenomena, especially those related to solar radiation, produce evident modifications in the mechanical response of laminated glass interlayer and can make pointless, over time, accurate numerical evaluations of mechanical response of laminated glass structures.

Acknowledgements

Acknowledgements: This research was partially financed by the Italian Ministry of Instruction and Research. The glass specimens were laminated by Roberglass Srl.

References

[1] Van Duser A, Jagota A, Bennison SJ. Analysis of glass/polyvinyl butyral laminates subjected to uniform pressure. Journal of Engineering Mechanics-Asce. 1999;125(4):435-42.
[2] Speranzini E, Agnetti S. Strengthening of glass beams with steel reinforced polymer (SRP). Composites Part B: Engineering. 2014;67(0):280-9.
[3] Foraboschi P. Analytical model for laminated-glass plate. Compos Pt B-Eng. 2012;43(5):2094-106.
[4] Galuppi L, Royer-Carfagni G. The effective thickness of laminated glass: Inconsistency of the formulation in a proposal of EN-standards. Compos Pt B-Eng. 2013;55:109-18.
[5] Newmark NM, Siess CP, I.M. V. Tests and analysis of composite beams with incomplete interaction. Proceedings of society for experimental stress analysis1951. p. 75-92.
[6] Contrafatto L, Cuomo M, Fazio F. An enriched finite element for crack opening and rebar slip in reinforced concrete members. International Journal of Fracture. 2012;178(1-2):33-50.
[7] Andreozzi L, Briccoli Bati S, Fagone M, Ranocchiai G, Zulli F. Dynamic torsion tests to characterize the thermo-viscoelastic properties of polymeric interlayers for laminated glass. Construction and Building Materials. 2014;65:1-13.
[8] Briccoli Bati S, Fagone M, Ranocchiai G, Romoli L. The influence of the interlayer on the behaviour of laminated glass in the serviceability domain. Glass Performance Days. Tampere, Finland2009. p. 722-5.
[9] El-Din NMS, Sabaa MW. Thermal degradation of poly(vinyl butyrral) laminated safety glass. Polymer Degradation and Stability. 1995;47(2):283-8.
[10] Saad GR, El-Shafee E, Sabaa MW. Dielectric and mechanical properties in the photodegradation of poly(vinyl butyral) films. Polymer Degradation and Stability. 1995;47(2):209-15.
[11] Liu R, He B, Chen X. Degradation of poly(vinyl butyral) and its stabilization by bases. Polymer Degradation and Stability. 2008;93(4):846-53.
[12] UNI_EN_ISO_12543-4:2011. Glass in building - Laminated glass and laminated safety glass: Test methods for durability. 2011.
[13] Delincé D, Belis J, Zarmati G, Parmentier B. Structural behaviour of laminated glass elements – a step towards standardization. Glass Performance Days. Tampere, Finland2007. p. 658-63.
[14] Ensslen F. Tragverhalten von bewitterten Verbund-Sicherheitsglas-Scheiben. Stahlbau. 2007;76(8):582-90.
[15] Weller B, Kothe M. Ageing Behaviour of Polymeric Interlayer Materials and Laminates. Glass Performance Days. Tampere, Finland2011. p. 240-3.
[16] Kothe M, Weller B. Influence of environmental stresses to the ageing behaviour of interlayer. In: Louter C, Bos F, Belis J, Lebet J-P, editors. Challenging glass 4 & COST action TU0905 final conference. Losanna: CRC PRESS-TAYLOR & FRANCIS GROUP; 2014.
[17] Louter C, Belis J, Veer F, Lebet JP. Durability of SG-laminated reinforced glass beams: Effects of temperature, thermal cycling, humidity and load-duration. Construction and Building Materials. 2012;27(1):280-92.

[18] Butchart C, Overend M. Influence of Moisture on the Post-fracture Performance of Laminated Glass. Glass Performance Days2013. p. 59-61.
[19] Serafinavicius T, Lebet J-P, Louter C, Kuranovas A, Lenkimas T. The effects of environmental impacts on durability of laminated glass plates with interlayers (SG, EVA, PVB). In: Louter C, Bos F, Belis J, Lebet J-P, editors. Challenging glass 4 & COST action TU0905 final conference. Losanna: CRC PRESS-TAYLOR & FRANCIS GROUP; 2014.
[20] Andreozzi L, Briccoli Bati S, Fagone M, Ranocchiai G, Zulli F. Test methods for the determination of interlayer properties in laminated glass: an overview. 12th ESG Conference. Parma, Italy2014.
[21] Christensen RM. Theory of Viscoelasticity, Second Edition: Dover Civil and Mechanical Engineering; 1982.
[22] Ferry JD. Viscoelastic properties of polymers. New York: John Wiley & Sons; 1980.
[23] Morrison FA. Understanding Rheology: Oxford UP 2001.
[24] Becker GW. Advanced experimental methods for mechanical properties of polymers. Materie Plastiche ed Elastomeri. 1969;35(1387).
[25] Macosko CW. Rheology: Principles, measurements, and applications. New York: Wiley; 1994.
[26] Ward IM. Mechanical Properties of solid polymers, 2nd. ed.: Wiley; 1990.
[27] Augier S, Coiai S, Passaglia E, Ciardelli F, Zulli F, Andreozzi L, et al. Structure and rheology of polypropylene with various architectures prepared by coagent-assisted radical processing. Polymer International. 2010;59(11):1499-505.
[28] Zulli F, Andreozzi L, Passaglia E, Augier S, Giordano M. Rheology of long-chain branched polypropylene copolymers. Journal of Applied Polymer Science. 2013;127(2):1423-32.
[29] Andreozzi L, Galli G, Giordano M, Zulli F. A Rheological Investigation of Entanglement in Side-Chain Liquid-Crystalline Azobenzene Polymethacrylates. Macromolecules. 2013;46(12):5003-17.
[30] Andreozzi L, Castelvetro V, Faetti M, Giordano M, Zulli F. Rheological and thermal properties of narrow distribution poly(ethyl acrylate)s. Macromolecules. 2006;39(5):1880-9.
[31] Doi M, Edwards SF. The Theory of Polymer Dynamics, 2nd ed. Oxford: Clarendon Press; 1988.
[32] Larson RG, Sridhar T, Leal LG, McKinley GH, Likhtman AE, McLeish TCB. Definitions of entanglement spacing and time constants in the tube model. Journal of Rheology. 2003;47(3):809-18.
[33] Zulli F, Giordano M, Andreozzi L. Onset of entanglement and reptation in melts of linear homopolymers: consistent rheological simulations of experiments from oligomers to high polymers. Rheologica Acta. 2015;54(3):185-205.
[34] Martin JW, Nguyen T, Byrd E, Dickens B, Embree N. Relating laboratory and outdoor exposures of acrylic melamine coatings: I. Cumulative damage model and laboratory exposure apparatus. Polymer Degradation and Stability. 2002;75(1):193-210.
[35] prEN16612. Glass in building - Determination of the load resistance of glass panes by calculation and testing. 2013.
[36] Andreozzi L, Briccoli Bati S, Fagone M, Ranocchiai G, Zulli F. Mechanical characterization of viscous thermo elastic properties of a polymer interlayer by dynamic tests. XX Congresso dell'Associazione Italiana di Meccanica Teorica ed Applicata. Bologna2011. p. 1-8.
[37] Dhaliwal AK, Hay JN. The characterization of polyvinyl butyral by thermal analysis. Thermochimica Acta. 2002;391(1–2):245-55.
[38] Physical Properties of Polymers Handbook. Second Edition ed: Springer; 2007.
[39] Wu S. Chain structure and entanglement. Journal of Polymer Science Part B: Polymer Physics. 1989;27(4):723-41.
[40] Lomellini P, Lavagnini L. Molecular weight polydispersity effects on the melt viscoelasticity of styrene-acrylonitrile random copolymers. Rheologica Acta. 1992;31(2):175-82.
[41] Andreozzi L, Autiero C, Faetti M, Giordano M, Zulli F. Dynamics, fragility, and glass transition of low-molecular-weight linear homopolymers. Philosophical Magazine. 2008;88(33-35):4151-9.
[42] Plazek DJ, Ngai KL. Correlation of Polymer Segmental Chain Dynamics with Temperature-Dependent Time-Scale Shifts. Macromolecules. 1991;24:1222-4.
[43] Huang D, McKenna GB. New insights into the fragility dilemma in liquids. The Journal of Chemical Physics. 2001;114(13):5621-30.
[44] Kunal K, Robertson CG, Pawlus S, Hahn SF, Sokolov AP. Role of Chemical Structure in Fragility of Polymers: A Qualitative Picture. Macromolecules. 2008;41(19):7232-8.

[45] Dalle-Ferrier C, Niss K, Sokolov AP, Frick B, Serrano J, Alba-Simionesco C. The Role of Chain Length in Nonergodicity Factor and Fragility of Polymers. Macromolecules. 2010;43(21):8977-84.
[46] Elfadl AA, Herrmann A, Hintermeyer J, Petzold N, Novikov VN, Rössler EA. Molecular Weight Dependence of Fragility in Polymers. Macromolecules. 2009;42(17):6816-7.

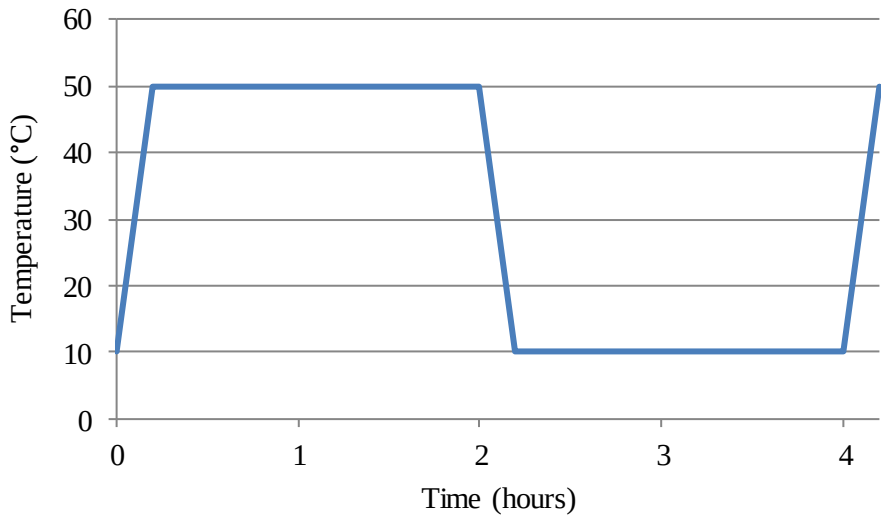

Figure 1. Thermal cycle.

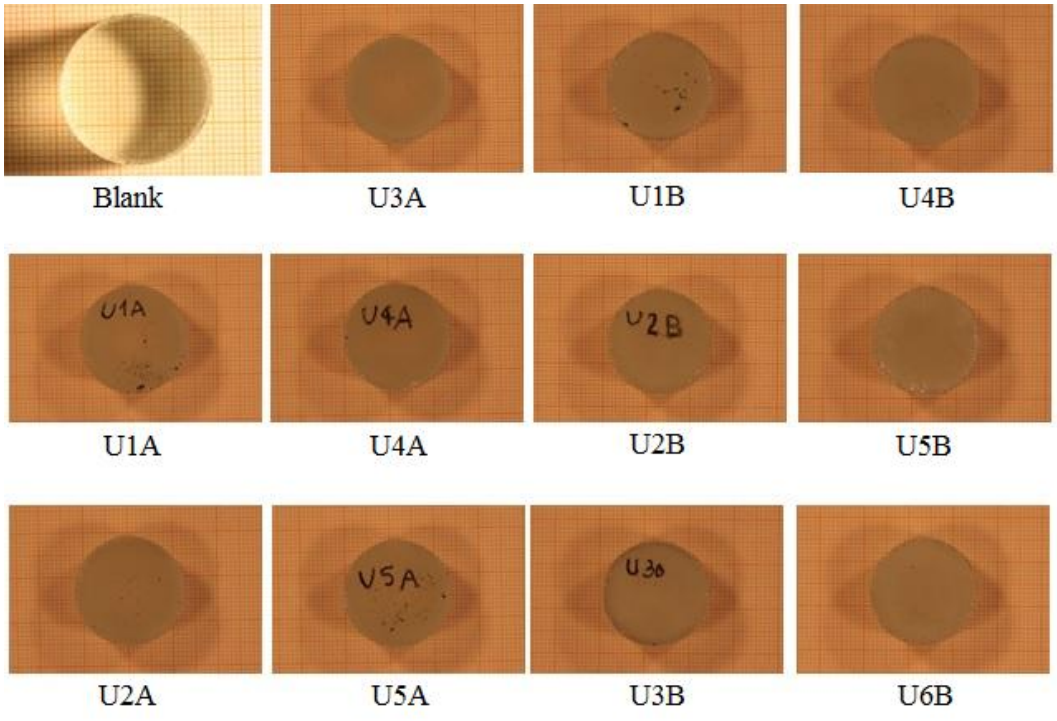

Figure 2. Specimens after 5425 hours of exposure to moisture: comparison with blank specimen PVB@0.76.

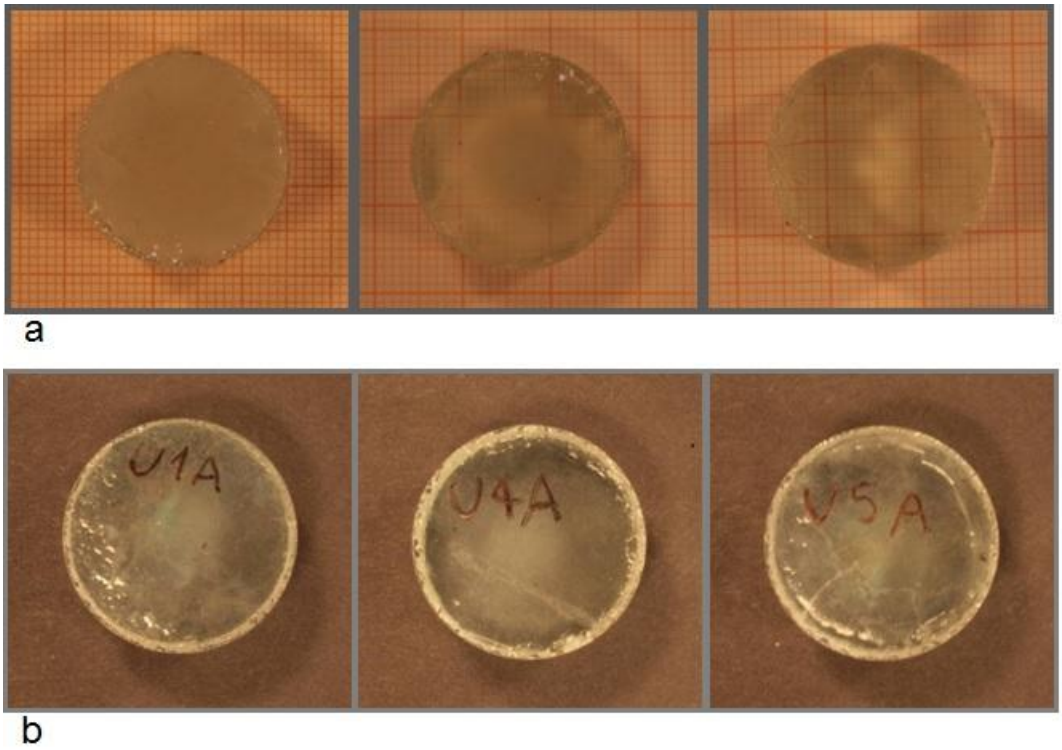

Figure 3. Specimens after humidity action: a. specimen U5B immediately after, two months after, six months after the end of absorption; b. specimens U1A, U4A and U5A affected by edge delamination after the moisture action.

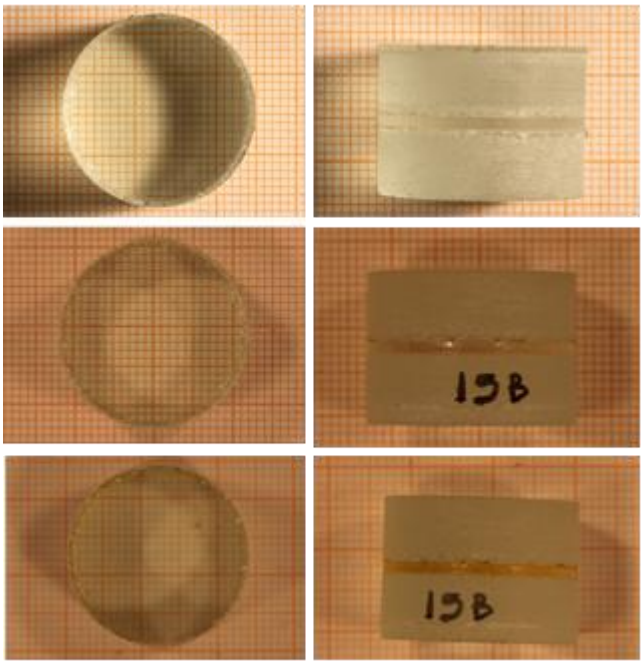

Figure 4. Comparison between a blank specimen and a specimen subjected to 5568 hours and to 11209 hours of exposure to radiation (Ultra-Vitalux® 300W).

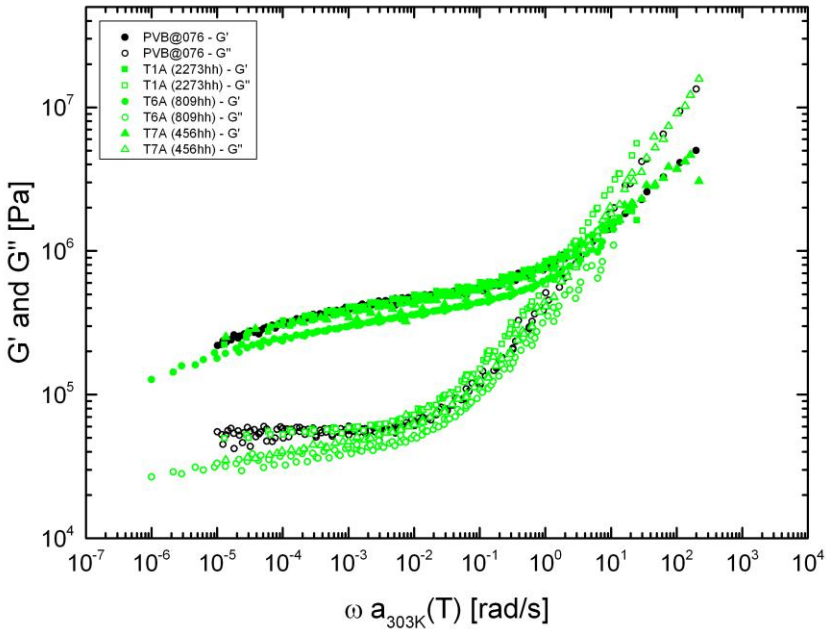

1

Figure 5. Master curves at T_r=30°C for specimens subjected to temperature cycles.

2

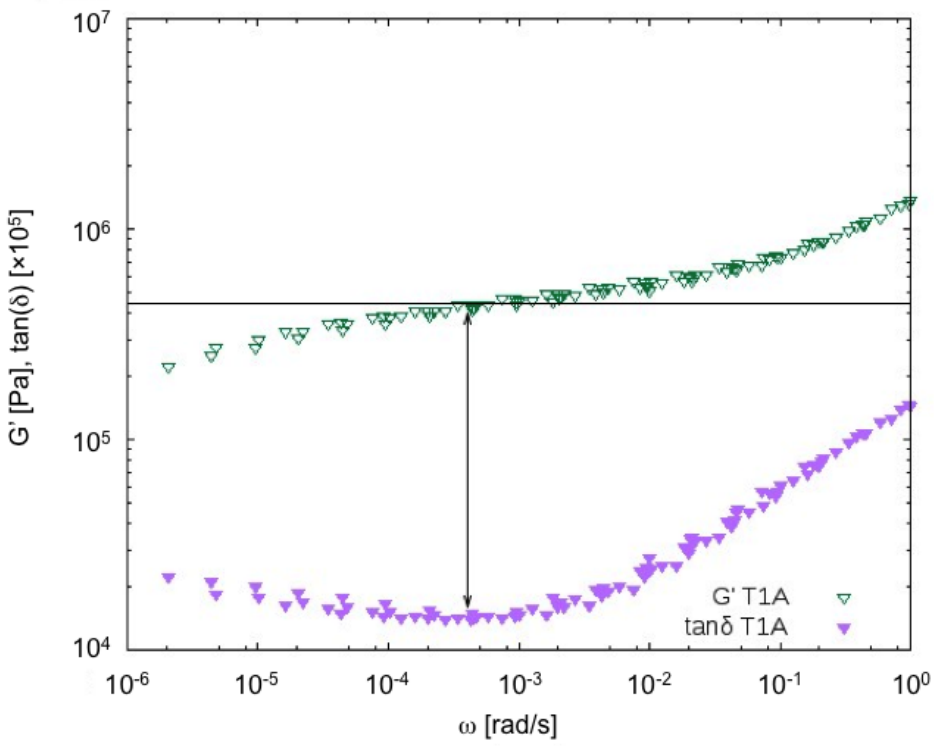

3

Figure 6. Determination of the plateau modulus G_N^0 for T1A specimen.

4

1

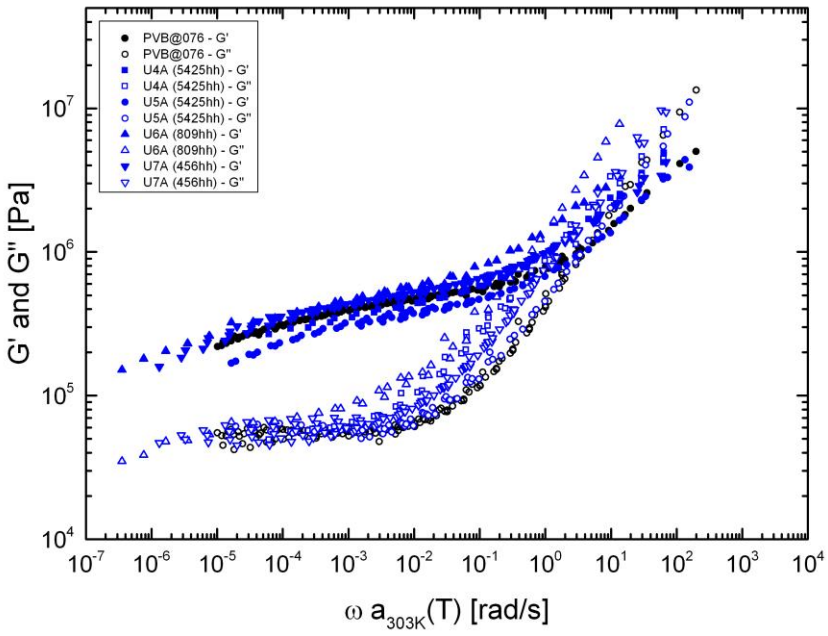

2

Figure 7. Master curves at T_r=30°C for specimens subjected to humidity action.

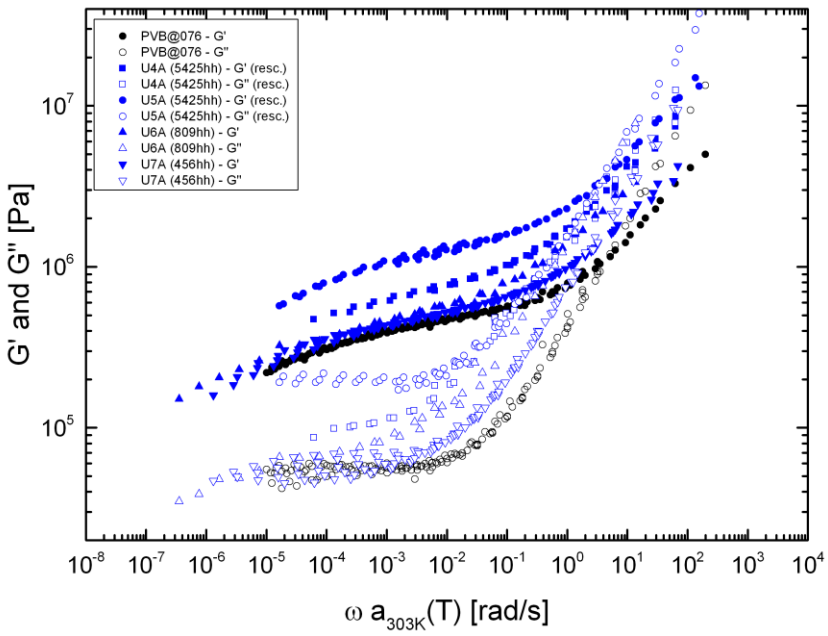

3

Figure 8. Master curves at T_r=30°C for specimens subjected to humidity action, rescaled for specimens U4A and U5A.

1

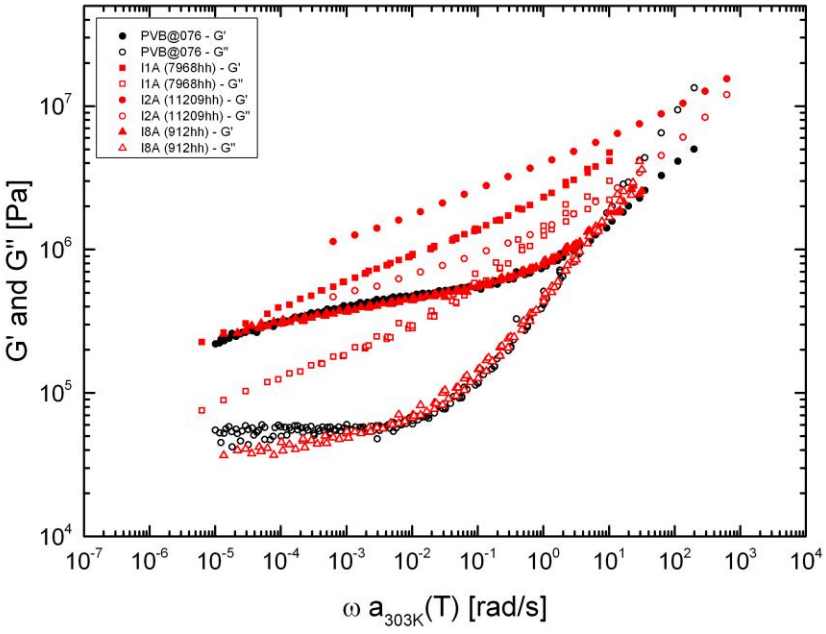

2

Figure 9. Master curves at T_r=30°C for specimens subjected to radiation action.

3

4

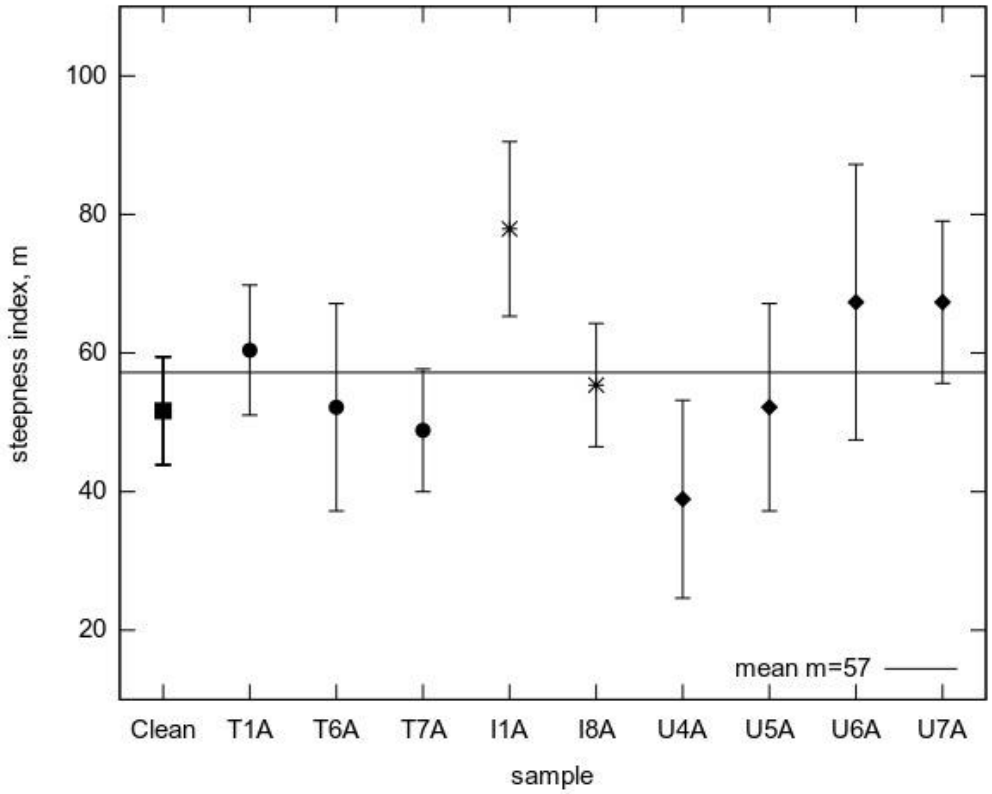

Figure 10. Steepness index *m*.

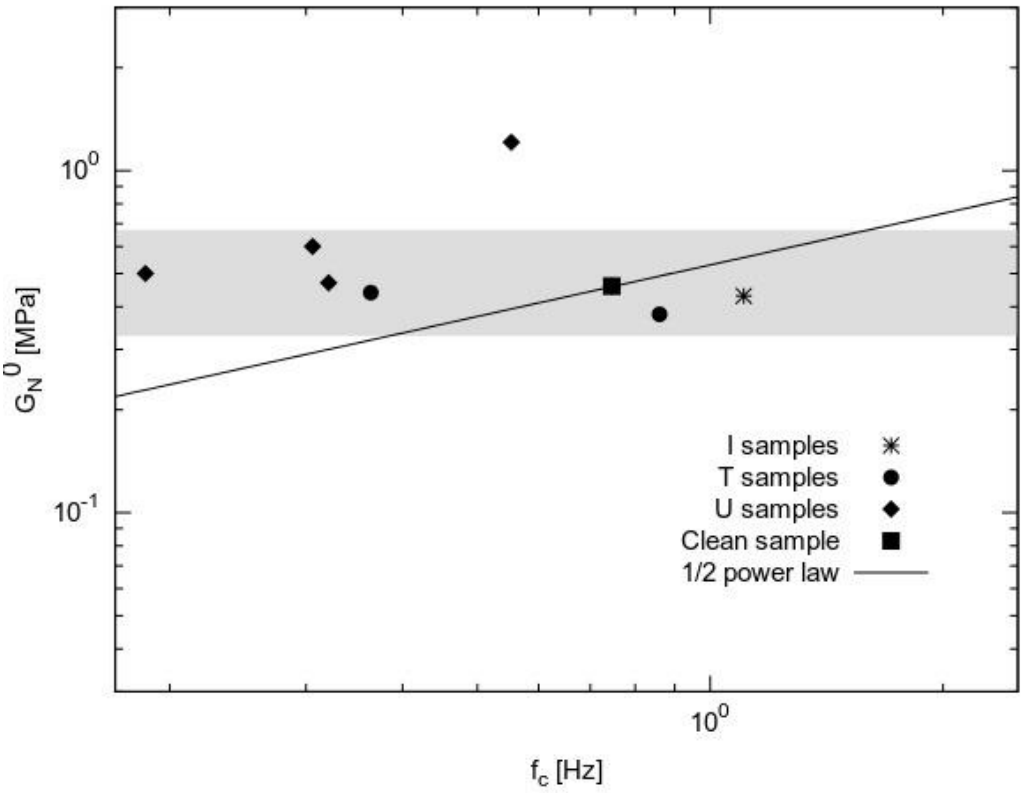

1

Figure 11. Plateau modulus as a function of crossover frequency; power law in agreement with [28].

Weathering action on thermo-viscoelastic properties of polymer interlayers for laminated glass

Laura Andreozzi[1], Silvia Briccoli Bati[2], Mario Fagone[2], Giovanna Ranocchiai[2], Fabio Zulli[1]

[1]*Department of Physics 'Enrico Fermi', University of Pisa, largo Bruno Pontecorvo 3, 56127 Pisa, Italy*

[2]*Department of Civil and Environmental Engineering, University of Florence, piazza F. Brunelleschi 6, 50121 Florence, Italy*

phone +390552756830

fax +39055212083

giovanna.ranocchiai@unifi.it

Highlights

- The effects of weathering have been produced on small laminated glass elements;
- Humidity action, solar radiation and thermal variation were simulated in laboratory, taking into account the relation between the produced artificial stress and the real weathering a composite glass structure could undergo.
- The use of small specimens enabled the repetition of mechanical tests for the analysis of the thermo-viscoelastic behaviour of interlayer, both on blank specimens and damaged ones.
- The effects of weathering action on the constitutive response of interlayer material was evaluated.
- The analysis of results permitted to make hypothesis on the structural changes that the material underwent at the molecular scale.

Figure 1

Click here to download high resolution image

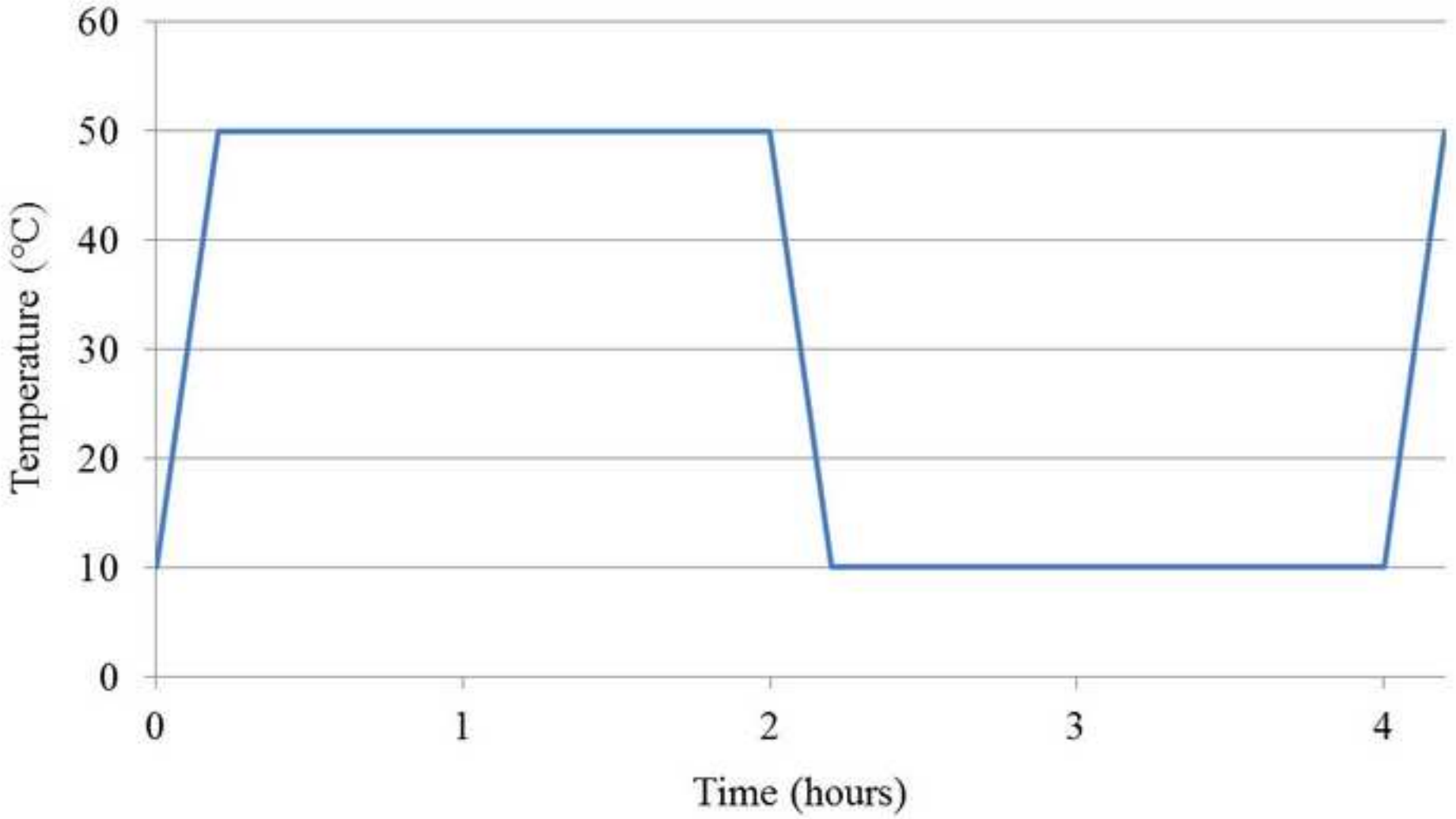

Figure 1

Click here to download high resolution image

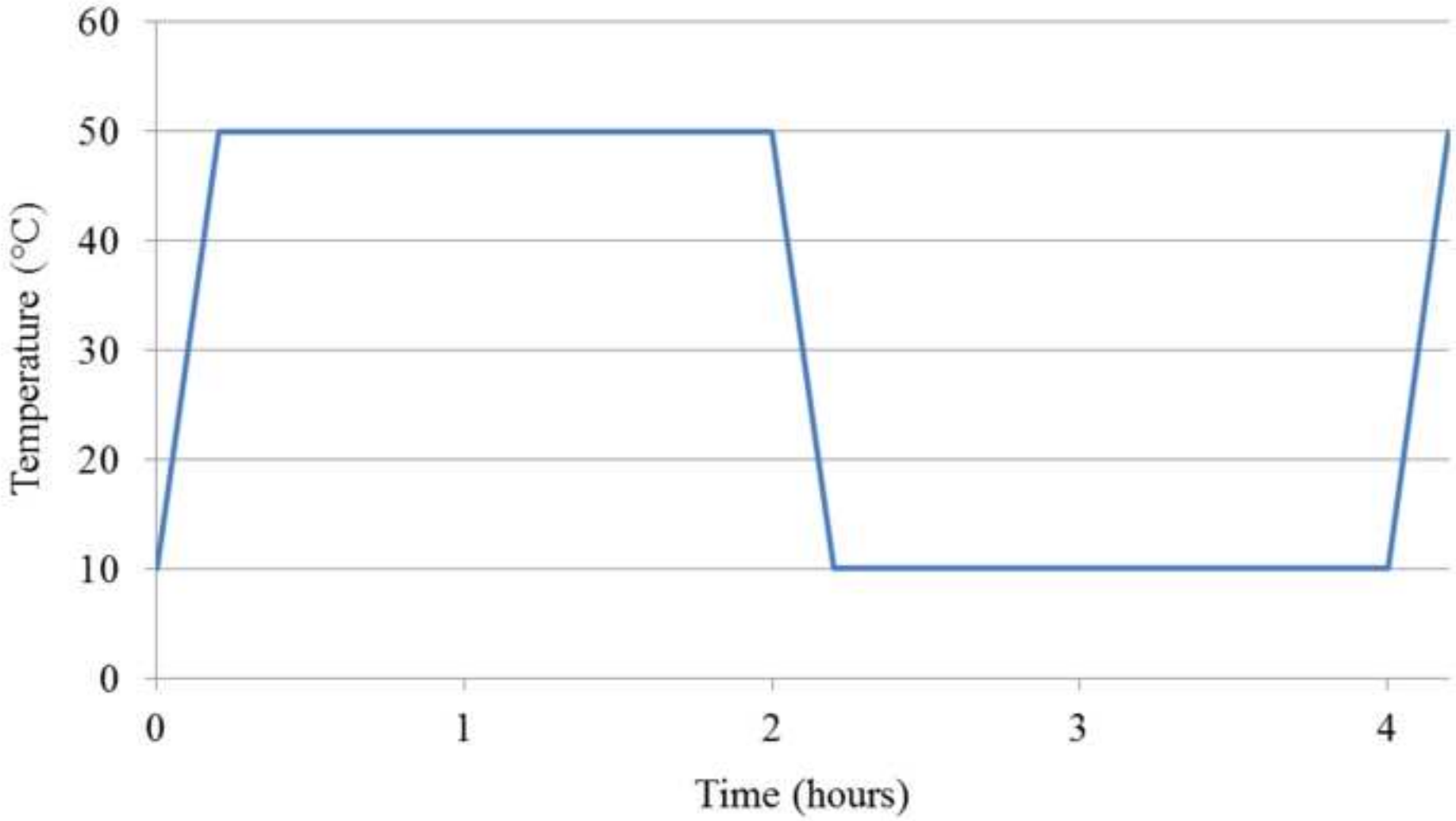

Figure 2

Click here to download high resolution image

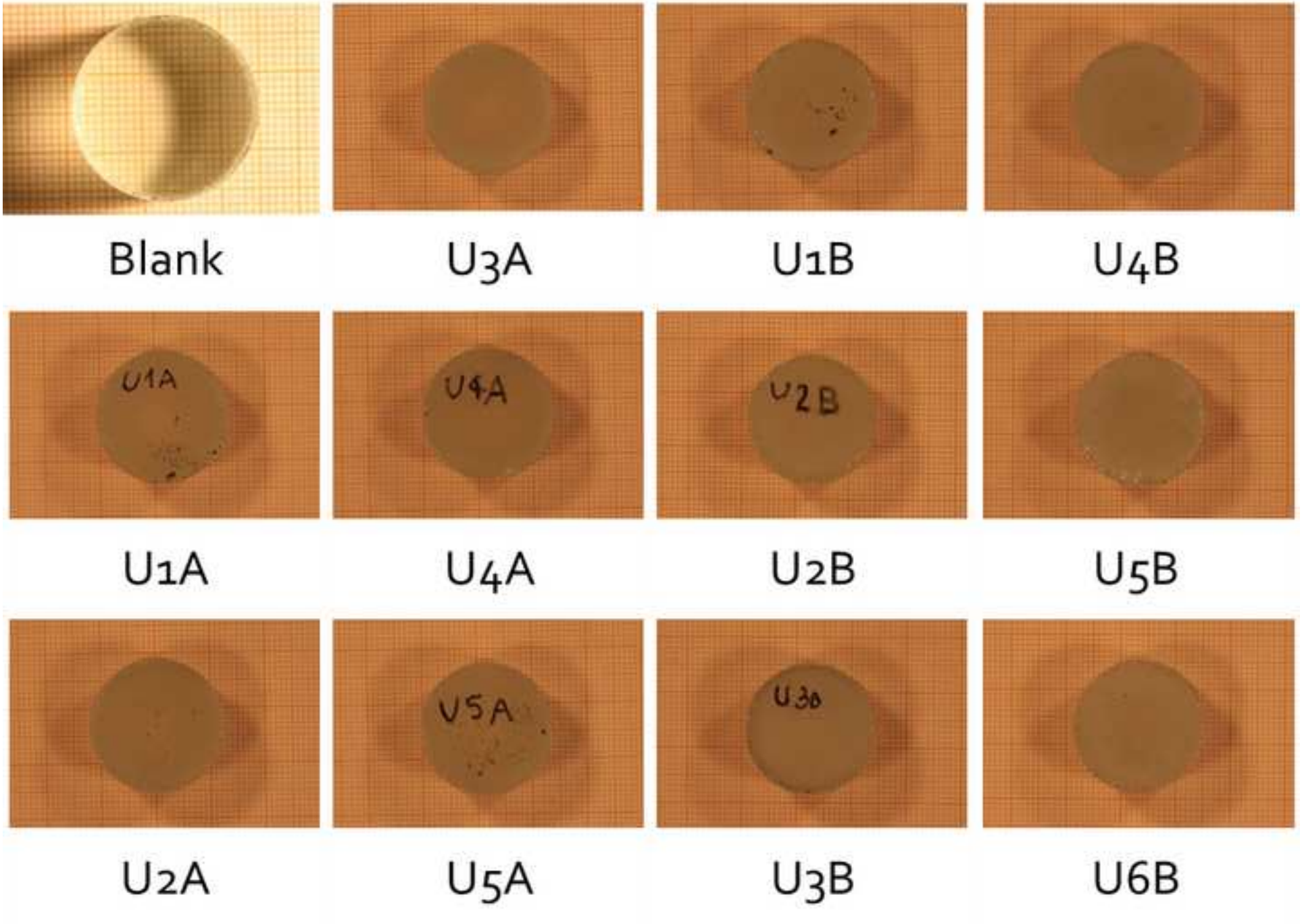

Figure 2

Click here to download high resolution image

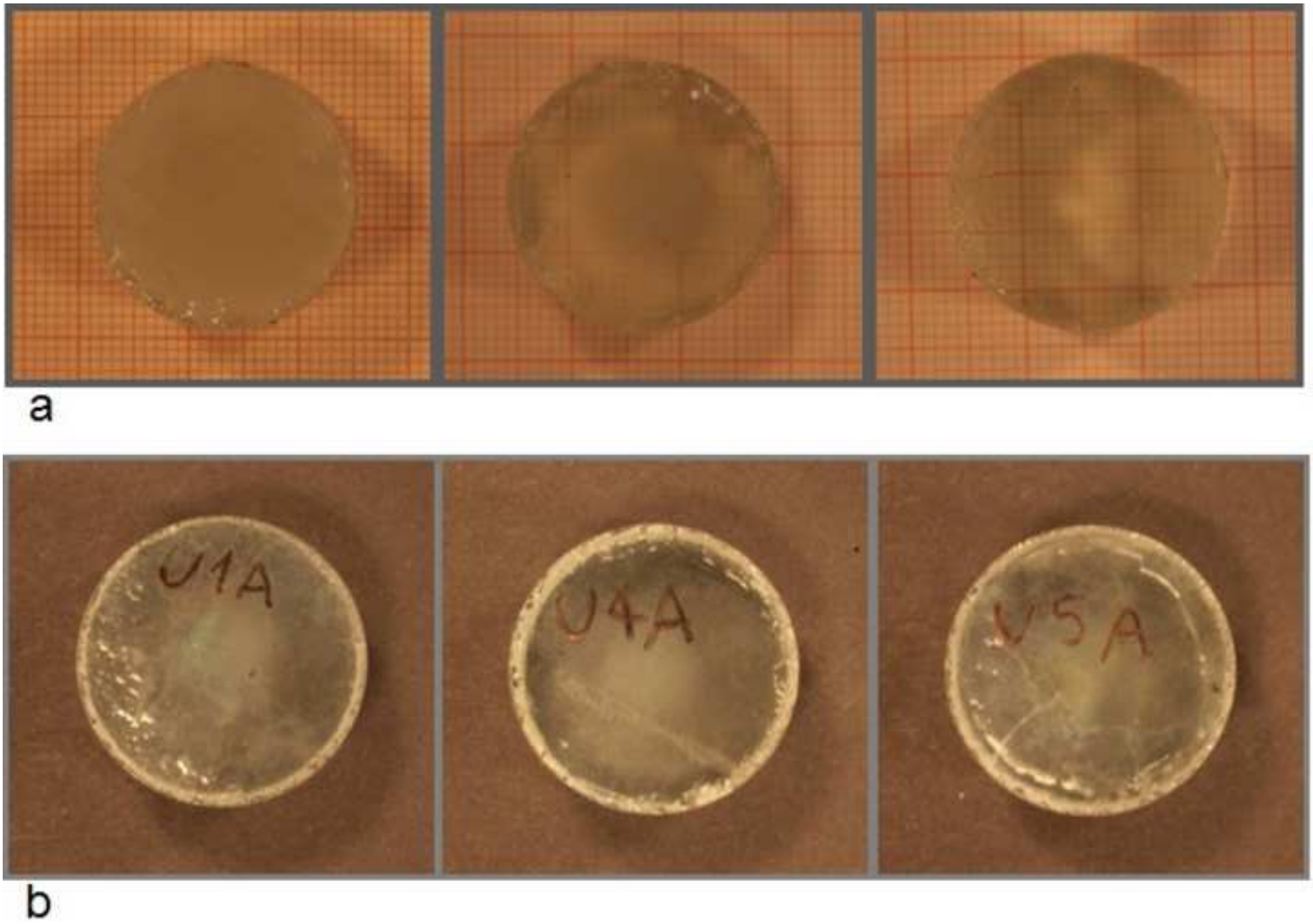

Figure 3

Click here to download high resolution image

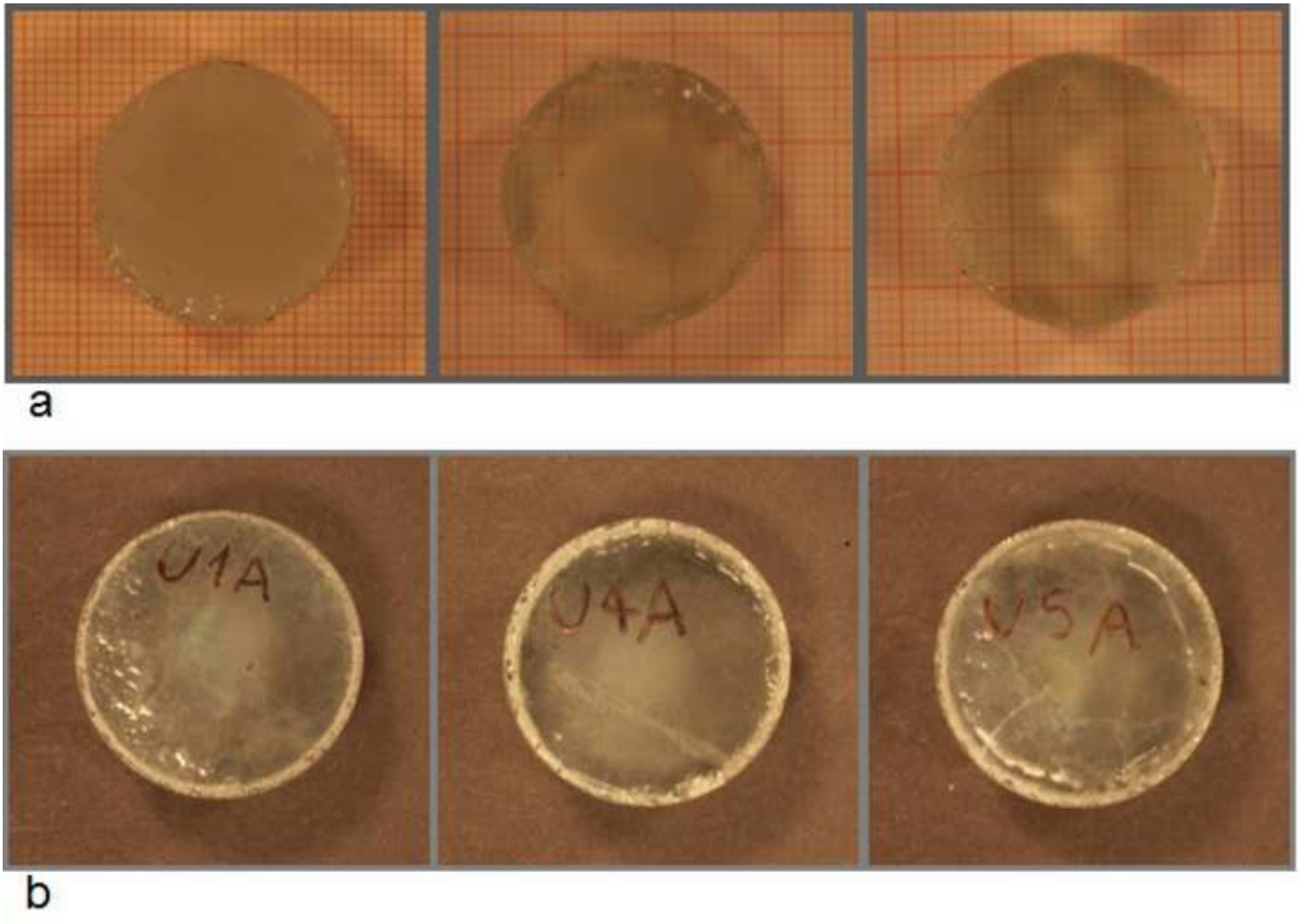

Figure 4

Click here to download high resolution image

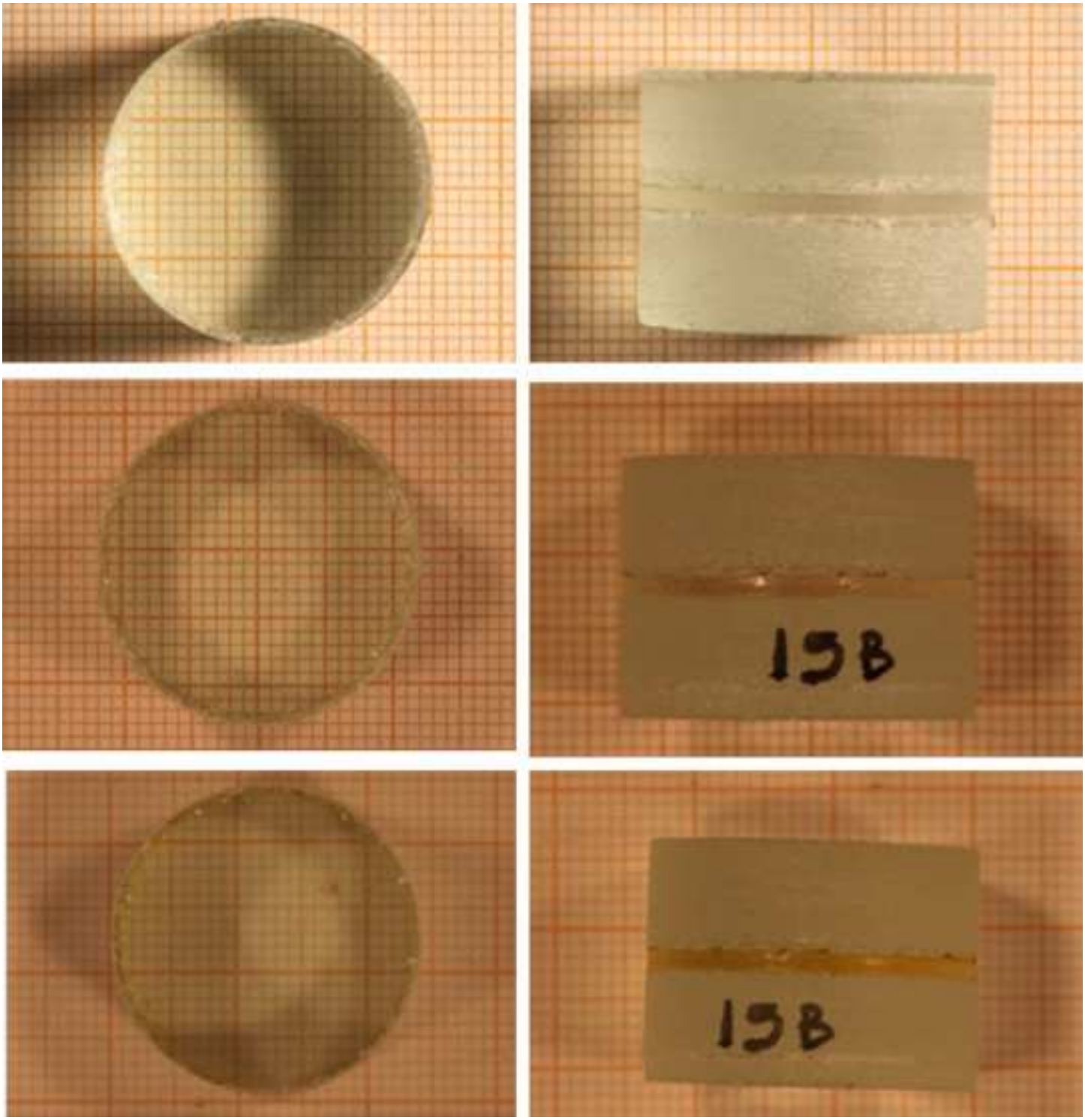

Figure 4

Click here to download high resolution image

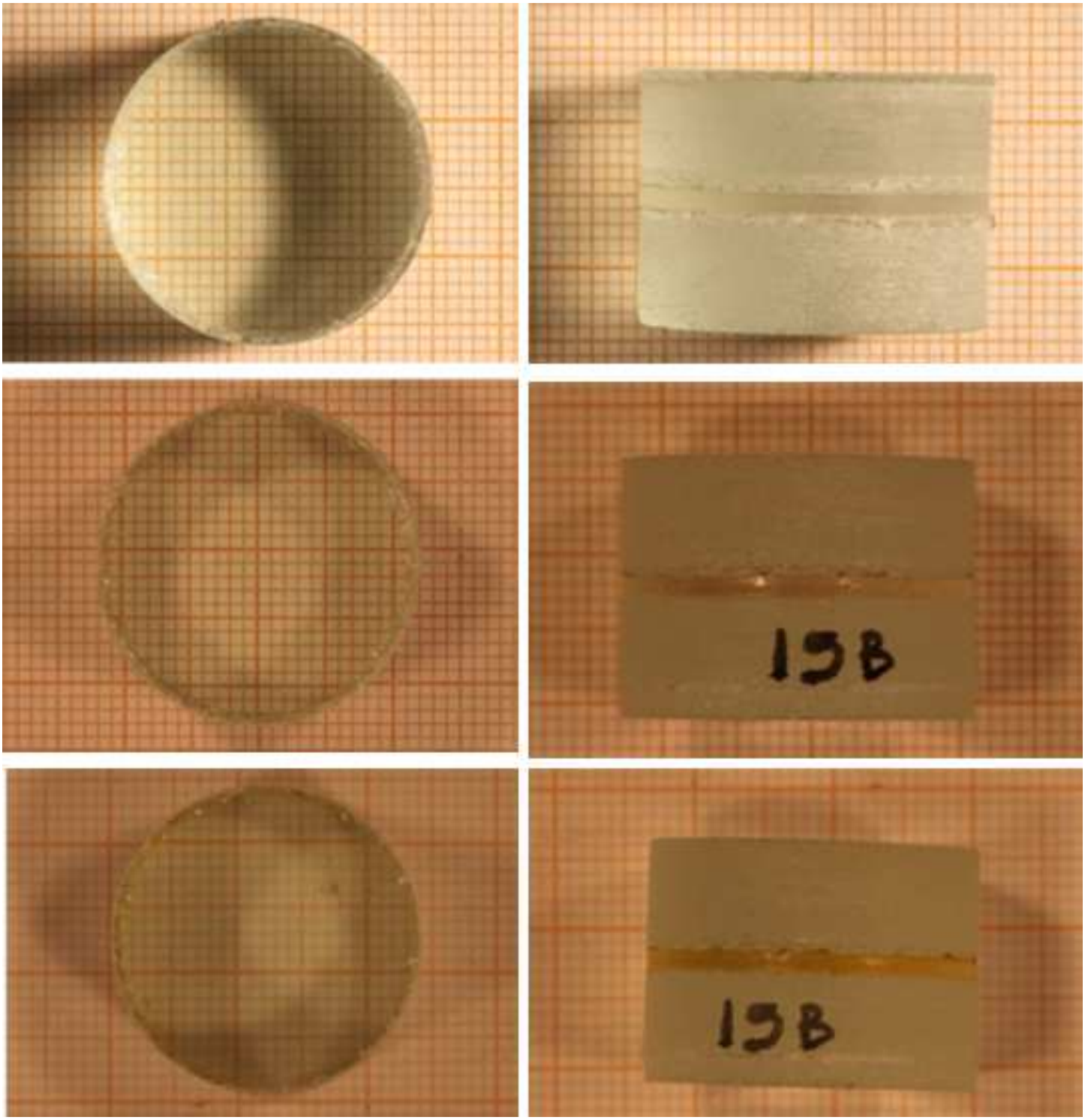

Figure 5

Click here to download high resolution image

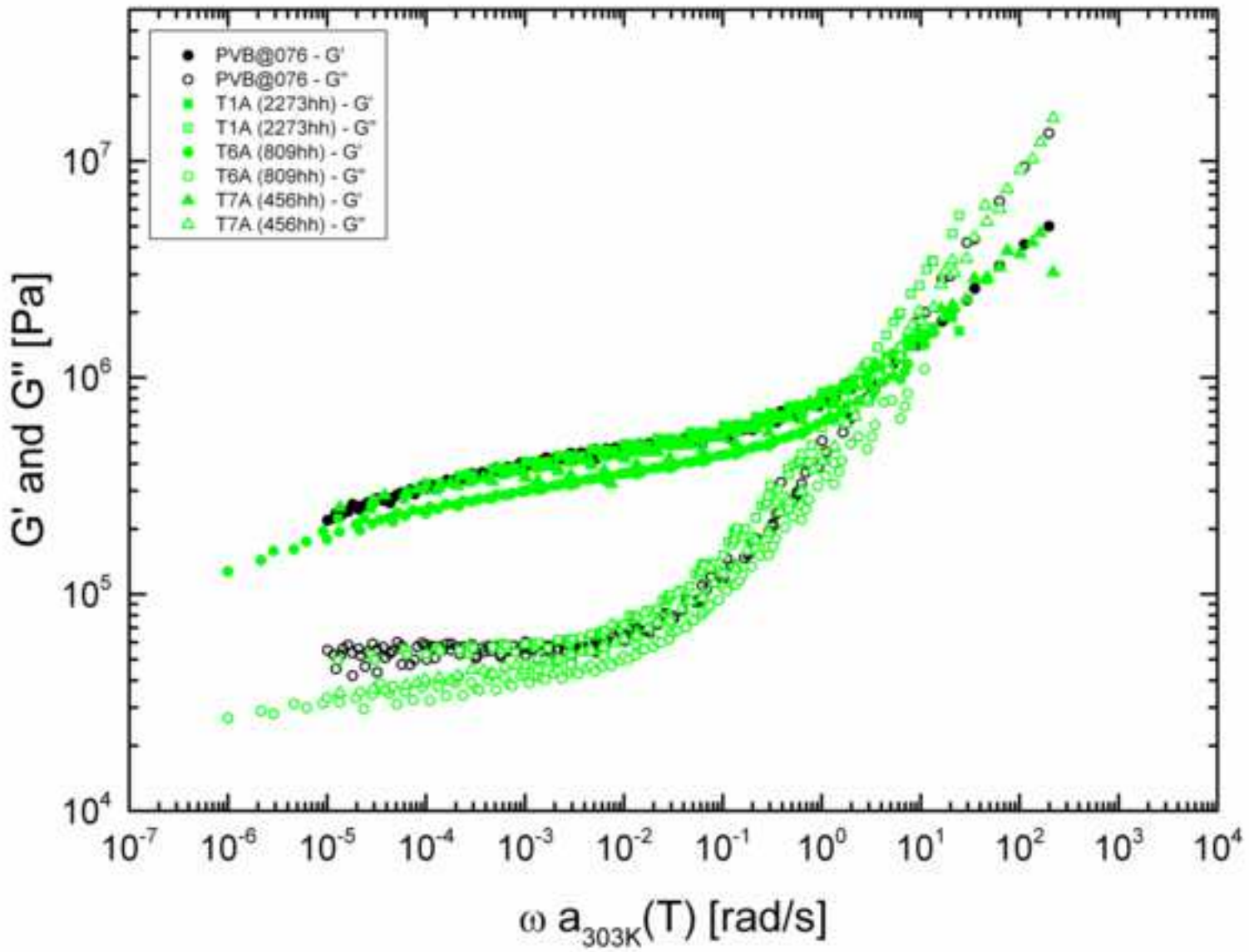

Figure 6

Click here to download high resolution image

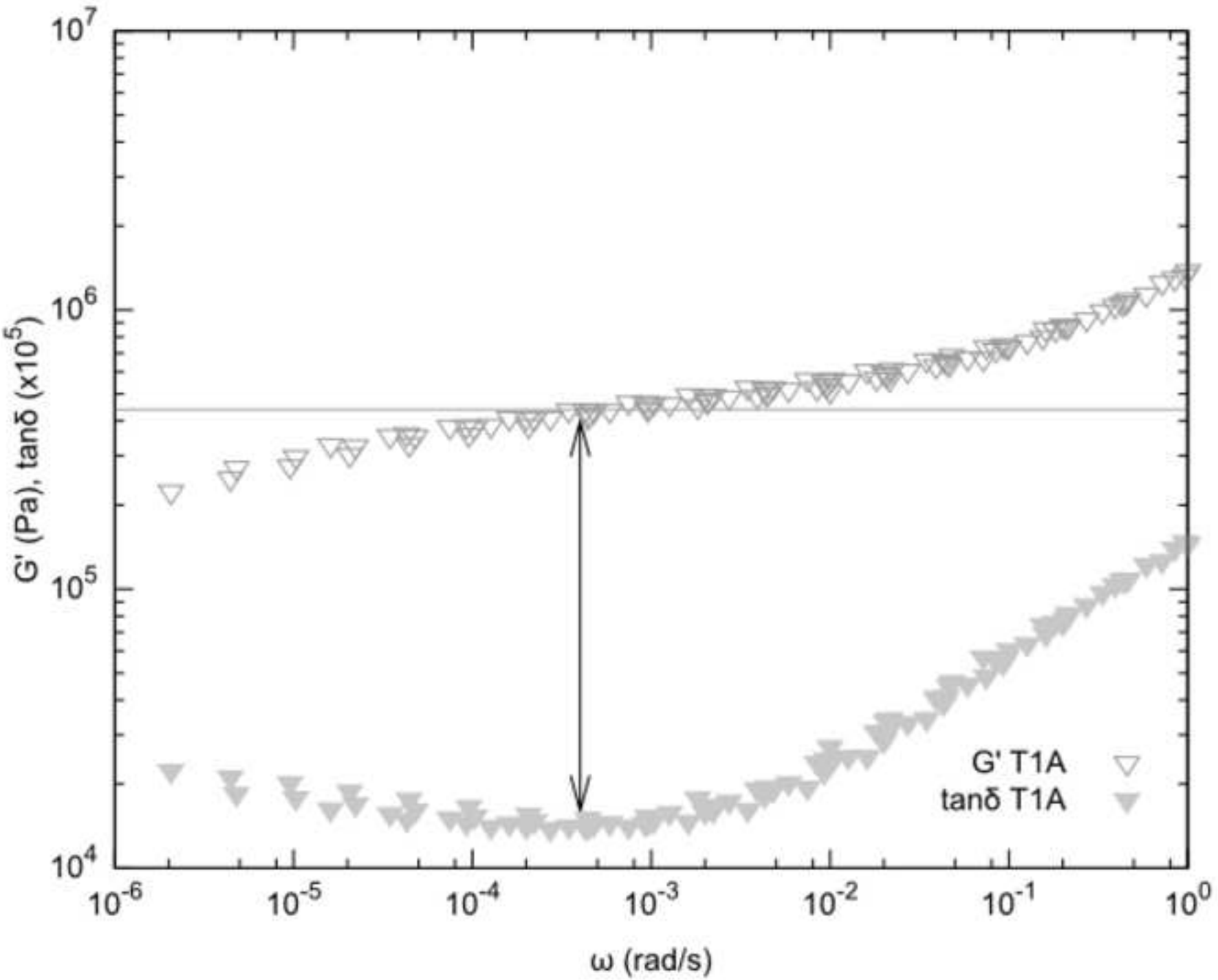

Figure 6

Click here to download high resolution image

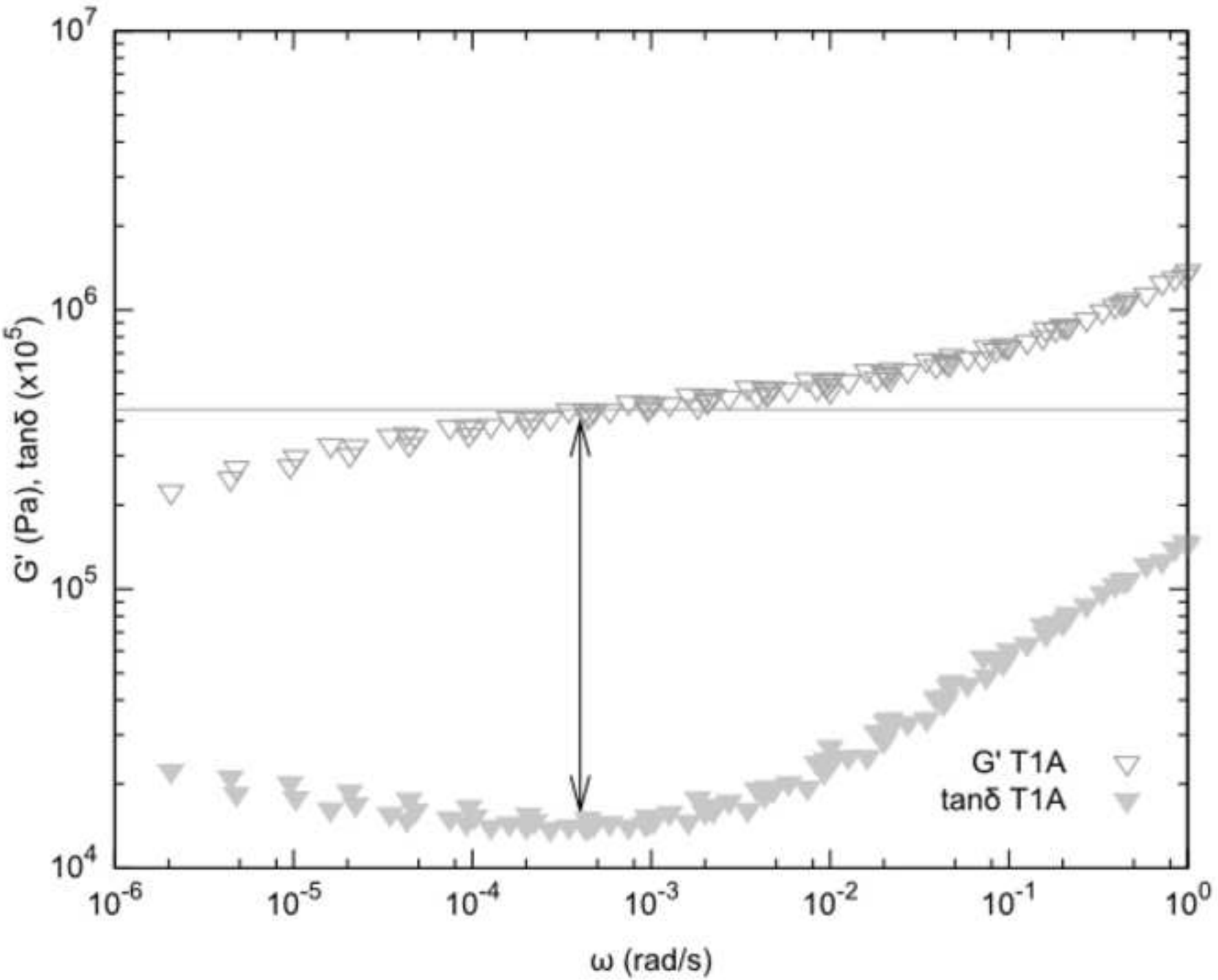

Figure 7

Click here to download high resolution image

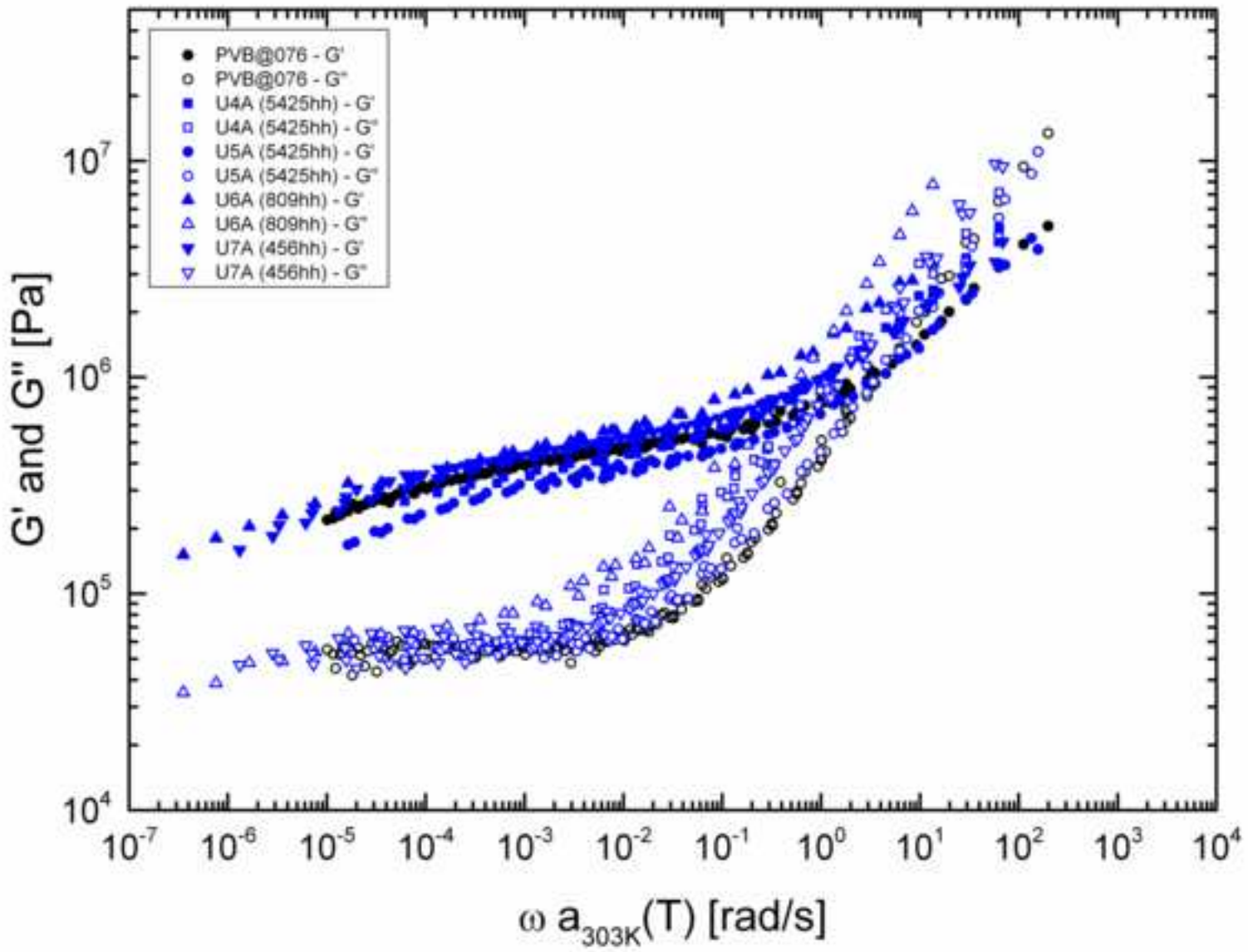

Figure 8

Click here to download high resolution image

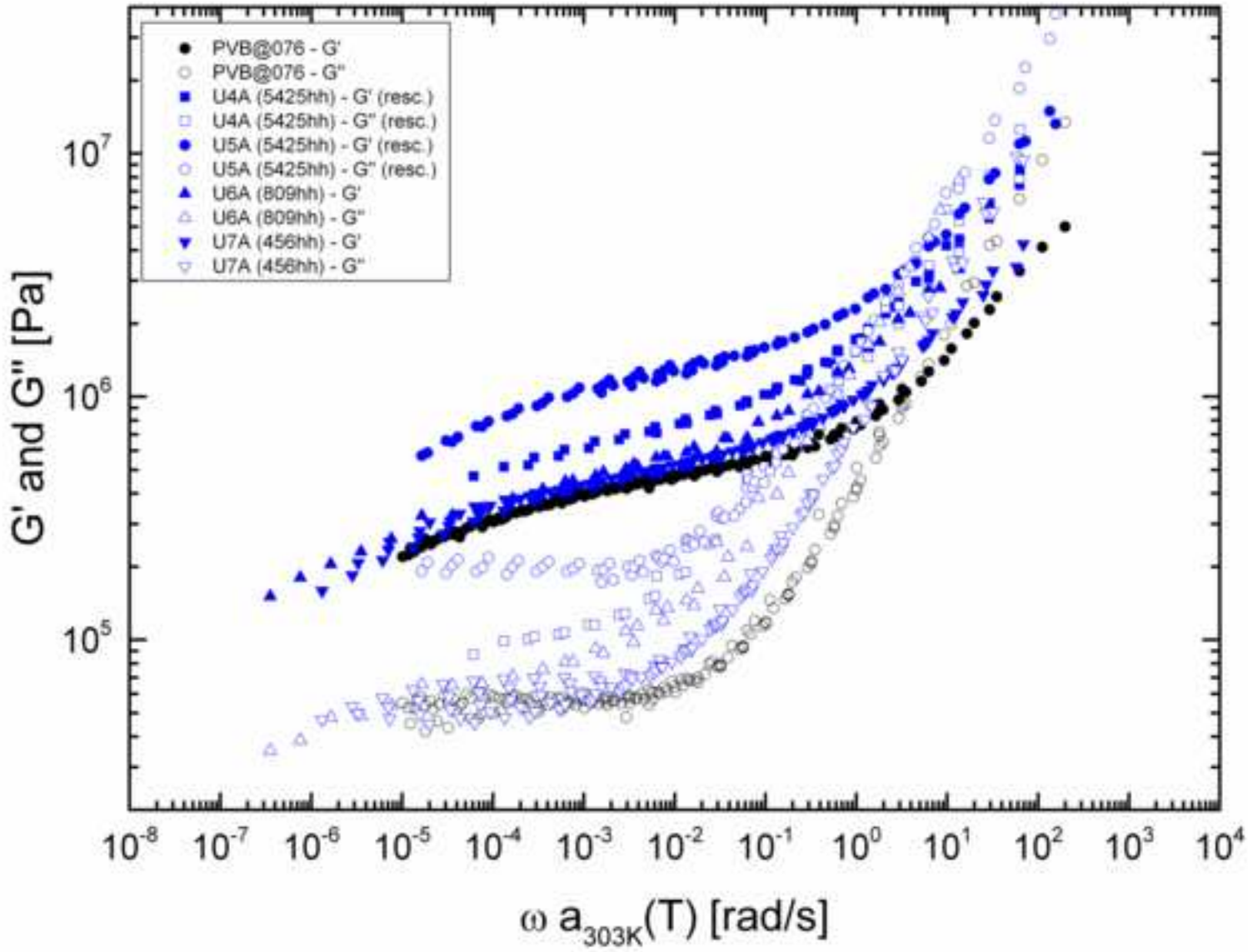

Figure 9

Click here to download high resolution image

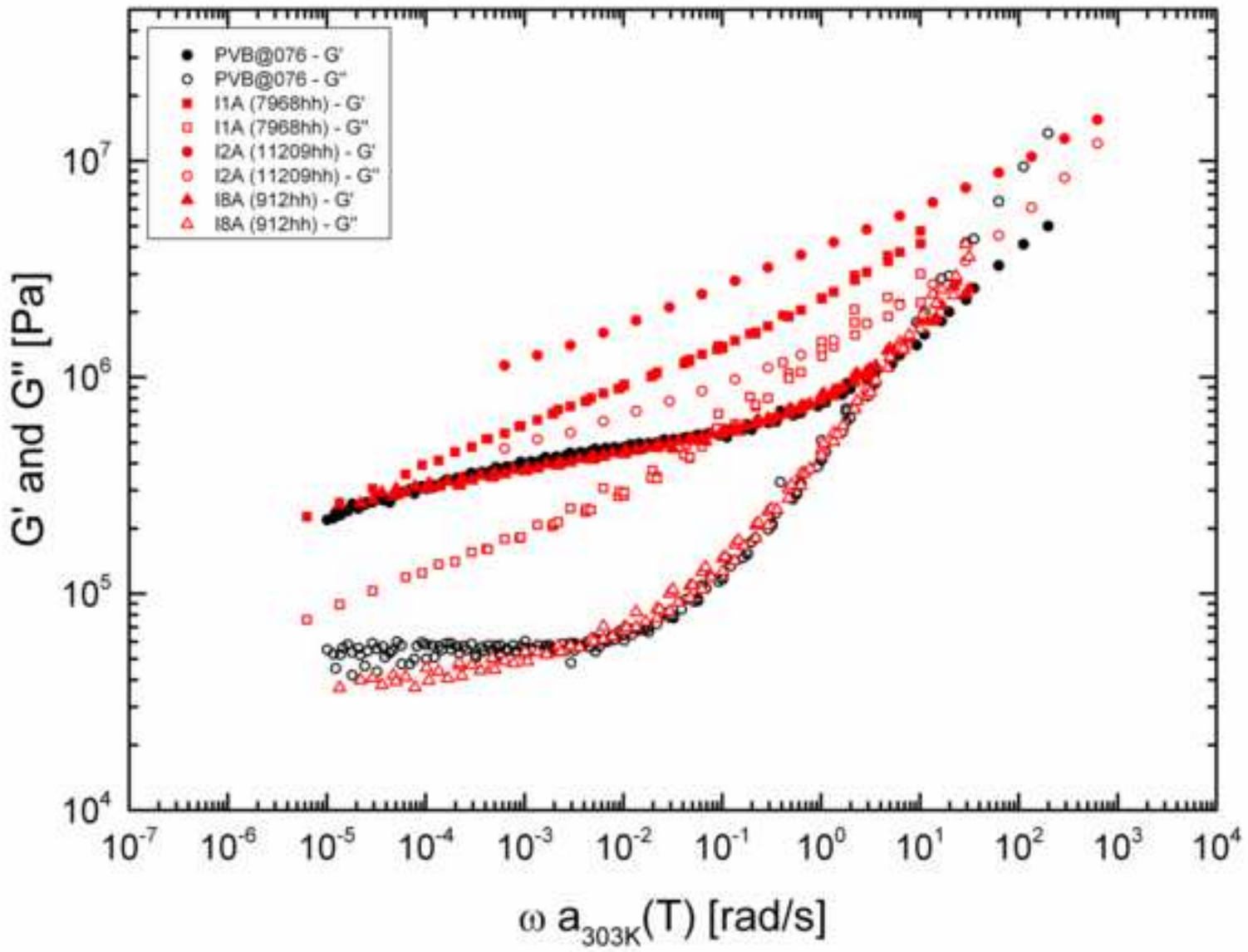

Figure 10

Click here to download high resolution image

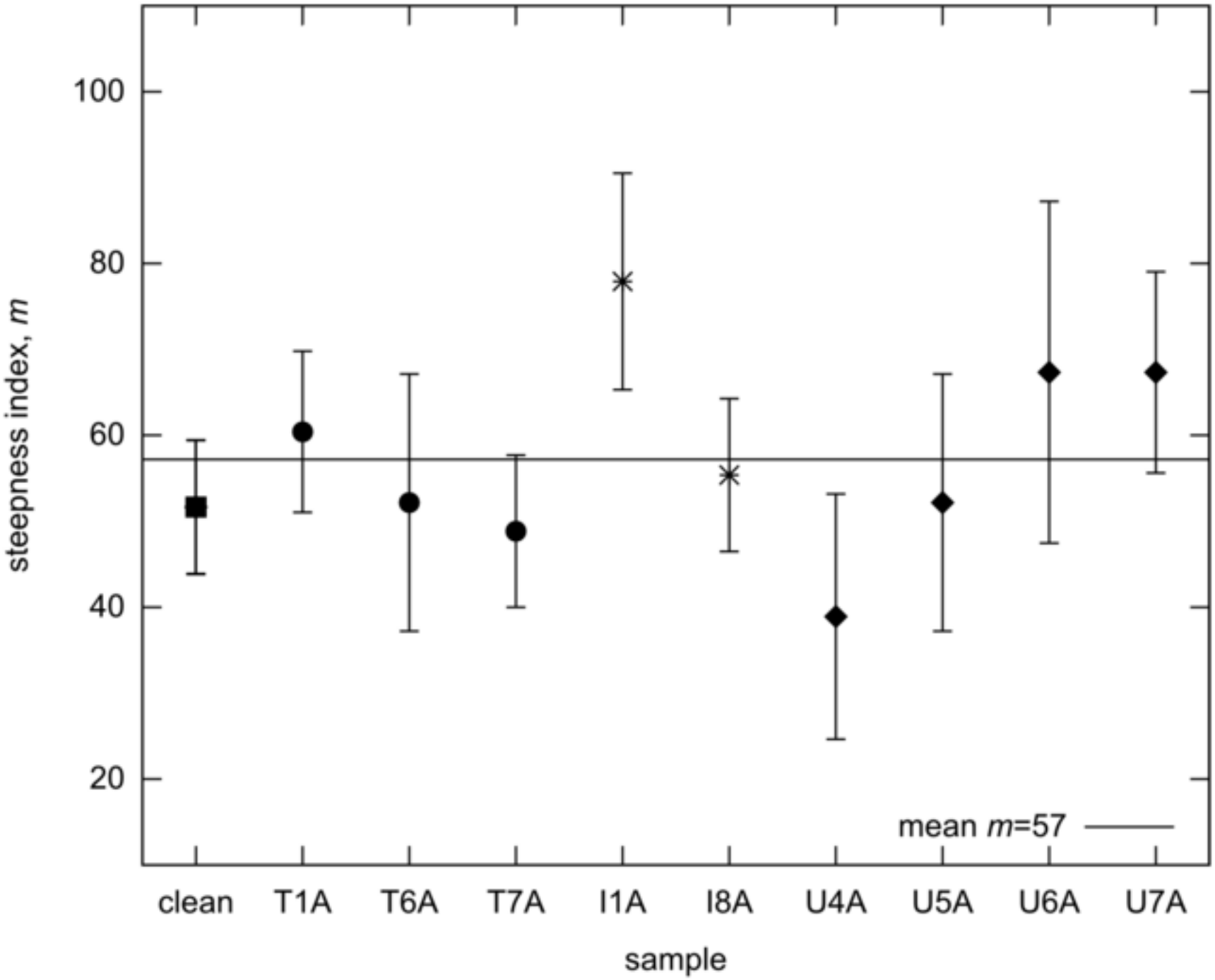

Figure 10

Click here to download high resolution image

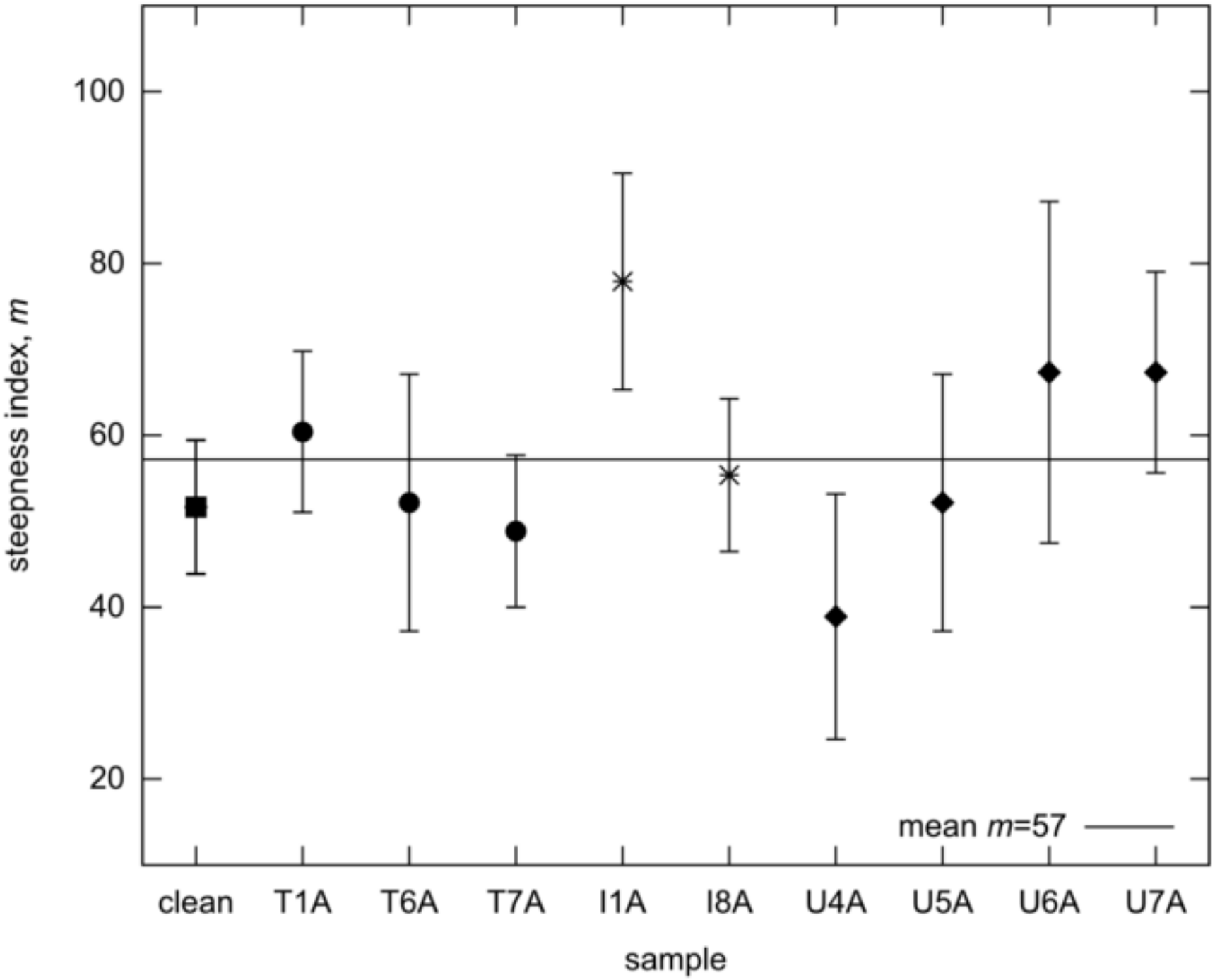

Figure 11

Click here to download high resolution image

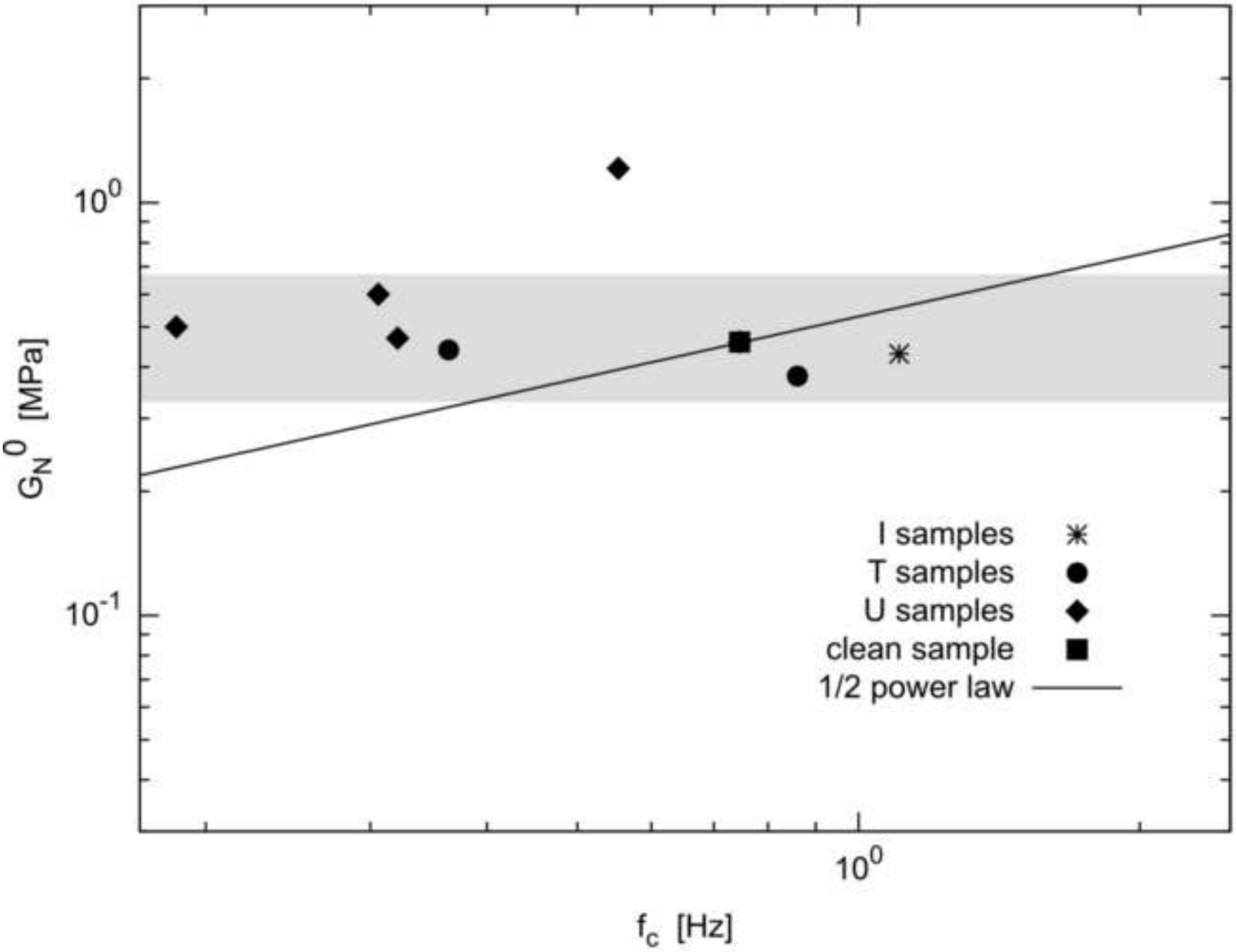

Figure 11

Click here to download high resolution image